THE JOURNAL OF PHYSICAL CHEMISTRY B

Article

Cite This: J. Phys. Chem. B 2018, 122, 6017−6032

pubs.acs.org/JPCB

Vapor Liquid Equilibria of Binary Mixtures of 1-Butyl-3-methylimidazolium Triflate (C_4mimTfO) and Molecular Solvents: *n*-Alkyl Alcohols and Water

Marcus Stuckenholz,[†] Emanuel A. Crespo,[‡] Lourdes F. Vega,[§] Pedro J. Carvalho,[‡] João A. P. Coutinho,[‡] Wolffram Schröer,[∥] Johannes Kiefer,[†] and Bernd Rathke*[,†]

[†]Universität Bremen, FB4, Technische Thermodynamik, Badgasteiner Strasse 1, 28359 Bremen, Germany

[‡]CICECO − Aveiro Institute of Materials, Department of Chemistry, University of Aveiro, 3810-193 Aveiro, Portugal

[§]Gas Research Center and Chemical Engineering Department, Khalifa University of Science and Technology, The Petroleum Institute, P.O. Box 2533, Abu Dhabi, United Arab Emirates

[∥]Universität Bremen, FB2, Institut für Anorganische und Physikalische Chemie, Leobener Strasse NWII, 28359 Bremen, Germany

Supporting Information

ABSTRACT: Isobaric vapor liquid equilibria (VLE) of binary mixtures of the ionic liquid (IL) 1-butyl-3-methylimidazolium trifluoromethanesulfonate (C_4mimTfO) with either water or short chained *n*-alkyl alcohols (methanol, ethanol, propan-1-ol, and butan-1-ol) are described in this study. Two different microebulliometers and a classical VLE apparatus were compared and the VLEs were determined in the composition range $0.4 \leq x(\text{solvent}) \leq 1$ at three different pressure levels (p = 500 mbar, 700 mbar, and 1000 mbar). The experimental data were modeled using the soft-SAFT equation of state, which was able to accurately describe the nonideal behavior of these mixtures. The combined experimental-modeling results obtained contribute to establish the structure−property relationship between the C_4mimTfO and *n*-alkyl alcohol molecules and to infer about its influence on the phase behavior of these solvents.

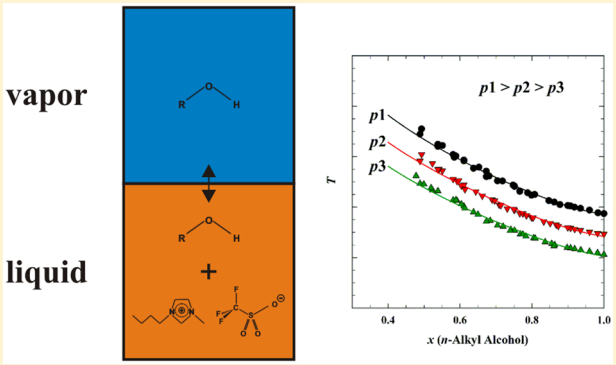

INTRODUCTION

In many industrial fields (e.g., chemical industry, food industry, or energy supply) low-temperature waste heat, with temperatures of about 330 K ≤ T ≤ 370 K, remains at the end of the process chain, with the heat being released in high amounts into the environment.[1,2] Absorption cycles (heat pumps, absorption chillers, or absorption transformers) are able to reuse this low grade waste heat economically, which results in an improvement of the primary energy efficiency.[3−5]

Generally, an absorption cycle uses a working pair consisting of two components. It consists of the refrigerant, with a high volatility and a low boiling point, and the absorbent, with a negligible volatility resulting in a high boiling temperature.[6] The most common working pairs are water and lithium bromide (H_2O/LiBr), which implies noncorroding plant design and a well-balanced process aiming at avoiding possible process operating problems due to crystallization,[7] and the ammonia and water (NH_3/H_2O) mixture with its inherent safety hazards.[3,6,8−11] Furthermore, aqueous mixtures work in a limited temperature range due to the freezing point of water-based mixtures.[6] These drawbacks illustrate the current demand for the development of alternative working pairs, suitable for a wider temperature range.[3,7] Besides, they should be less toxic or even environmentally friendly or, ultimately, green.[12−15] Recently, there has been a strong focus on the study of ionic liquids (ILs) mixtures for such applications as substitutes for the commonly used absorbents.[4]

ILs usually are organic salts composed by a large organic cation, with a dispersed charge, and an organic or inorganic anion. Hence, their molecular structure disturbs the high ordering typically found in, e.g., alkali halides, and decreases the electrostatic interactions resulting in lower melting temperatures around room temperature; boiling temperatures are typically above the stability limit, which is on the order of T = 500 K.[16−18] On top of these properties are their very low vapor pressures and in some cases a negligible flammability.[17,19] The thermophysical properties of ILs, such as, e.g., densities, viscosities, or melting points, can be tuned over a wide range by selecting suitable cation−anion pairs or liquid mixtures.[20] Due to their availability and relevance in science, the class of 1-alkyl-3-methylimidazolium based ILs was comprehensively but

Received: April 6, 2018
Published: May 7, 2018

DOI: 10.1021/acs.jpcb.8b03278
J. Phys. Chem. B 2018, 122, 6017−6032

randomly characterized so that about 75% of publications are focusing on this class of ILs.[20,21] In the field of working fluids for absorption cycles, binary mixtures of an IL and a suitable solvent became interesting. Related investigations focused on mixtures where the IL acts as a classical absorbent and the molecular solvent as the counterpart of a classical refrigerant. Most of these studies are related to mixtures of IL and water as potentially environmentally friendly working pairs for absorption cycles.[3,22−29] From a more general point of view, mixtures of ILs with other molecular liquids exhibiting good refrigerant properties were also considered as substitutes for the classical mixtures, like IL/NH_3,[30,31] IL/CO_2,[32−37] IL/N_2O,[38] IL/hydrofluorocarbons,[39−42] and IL/alcohols.[8,43−46] IL/alcohol mixtures stand out by showing high thermal stability, opening the possibility to work at output temperatures up to almost T = 500 K with a low risk of crystallization inside the process unit.[3] Albeit a larger number of studies focused on the determination of thermophysical properties, e.g., viscosities or densities,[17,26,47] systematic studies on the phase behavior of these mixtures are scarce. While in the past many investigations dealt with the liquid−liquid phase behavior,[48−60] a much smaller number of studies focused on vapor liquid equilibria (VLE).[44,61−72] Those focused on VLE were mainly performed applying classical VLE set-ups, stills, and ebulliometers; for an overview of the different experimental techniques see refs 25, 70, 71, and 73−77.

IL containing systems introduce additional problems to the VLE determination in classical stills due to increased viscosities, strongly depending on the composition of the mixtures, and due to a reduced volatility of one component, resulting in a reduced volume or even mass flow inside classical stills.[61] Equilibrium conditions during the ongoing determination of the VLE are hard to reach under such conditions. Therefore, investigations on VLEs of IL/alcohol mixtures are scarce,[44,61] even though alcohols are also promising candidates for such applications due to their thermal stability.[3,78]

Therefore, in this work, a systematic study on the vapor liquid equilibria of binary mixtures was conducted. The components were selected with the preference to allow for a gradual variation of the thermodynamic properties of the more volatile component. For this purpose, the ionic liquid 1-butyl-3-methlyimidazolium trifluoromethanesulfonate (C_4mimTfO) and the n-alkyl alcohols (C_nOH, n = 1−4) were selected. The experiments were performed using an isobaric microebulliometer, which is validated by the determination of the VLE of mixtures of C_4mimTfO and H_2O under conditions chosen in a prior study by Passos et al.[22] In order to contribute to the debate, if a miniaturization of a VLE apparatus may hamper the experimental results systematically, we have performed a direct comparison between the microebulliometer and a classical commercial VLE apparatus, which was developed on the basis of the pioneering work by Cottrell,[79] Gillespie,[80] Hala and Wichterle,[81,82] and Stage and Müller.[83−85] In the present work, we are reporting the VLE of five different mixtures of C_4mimTfO with water and the n-alkyl alcohols C_nOH; n = 1−4. Results are discussed in terms of the modified Raoult's law and the activity coefficients derived from the mixtures' boiling points. Systematic changes are described against the background of structure property relationships and compared with the results obtained using the soft-SAFT model,[86,87] a molecular-based EoS based on statistical thermodynamics, which is able to explicitly account for different structural and energetic effects, such as hydrogen bonding, that play a vital role in complex systems such as those involving ionic liquids. Soft-SAFT has already been used to characterize several ionic liquids in excellent agreement with experimental data.[88−91]

EXPERIMENTAL SECTION

Materials and Sample Preparation. The ionic liquid 1-butyl-3-methylimidazolium trifluoromethanesulfonate ($C_9H_{15}F_3N_2O_3S$, C_4mimTfO, CAS-No. 174899-66-2, purity mass fraction $w(C_4\text{mimTfO}) \geq 0.99$; (chemical structure depicted in Figure 1)) was purchased from IoLiTec (Ionic Liquids Technologies GmbH, Heilbronn, Germany). Volatile compounds were removed under reduced pressure ($p < 5 \times 10^{-2}$ mbar) and constant stirring at ambient temperature for a minimum of 24 h; no further mass loss was detected after this time.

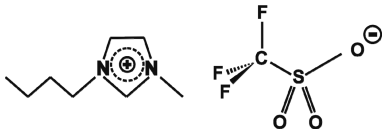

Figure 1. Chemical structure of the ionic liquid 1-butyl-3-methylimidazolium trifluoromethanesulfonate (C_4mimTfO).

The total water content was monitored by Karl Fischer titration and was less than $w(H_2O)$ < 100 ppm. The ionic liquid was handled in Duran culture tubes (V = 5 mL), sealed by 3-Layer Septa (silicone rubber, type 76006, Hamilton AG, Bonaduz, Switzerland), and fixed with GL 14 screw caps (Duran Group GmbH, Mainz, Germany).

The n-alkyl alcohols, methanol (C_1H_4O, CAS-No. 67-56-1, purity mass fraction $w(C_1OH) \geq 0.999$; C_1OH), ethanol (C_2H_6O, CAS-No. 64-17-5, purity mass fraction $w(C_2OH) \geq 0.998$; C_2OH), propan-1-ol (C_3H_8O, CAS-No. 71-23-8, purity mass fraction $w(C_3OH) \geq 0.998$; C_3OH), and butan-1-ol ($C_4H_{10}O$, CAS-No. 71-36-3, purity mass fraction $w(C_4OH) \geq 0.998$; C_4OH) were purchased from Merck ($C_{n=1,2,4}OH$; Merck KGaA, Darmstadt, Germany) and Fluka/Sigma-Aldrich (C_3OH, Sigma-Aldrich Chemie GmbH, Munich, Germany), respectively. In order to avoid contamination of the components by ambient humidity, the liquids were handled under protective argon atmosphere (Ar 5.0, Air Liquide, Düsseldorf, Germany) inside a glovebox. The more volatile components used within this study were dried over molecular sieves (3 Å, Merck KGaA, Darmstadt, Germany) for a minimum of 24 h. The n-alkyl alcohols propan-1-ol and butan-1-ol were additionally purified by vacuum distillation under reduced pressure (propan-1-ol: p = 667 mbar and T = 358 ± 0.5 K; butan-1-ol: p = 500 mbar and T = 371 ± 0.5 K) prior use. The water was double distilled (H_2O, CAS-No. 7732-18-5) and degassed prior to use.

Experimental Set-Up and Determination of VLE. The VLE of each liquid mixture was determined inside a glassy microebulliometer (Duran glass, Duran Group GmbH, Mainz, Germany) operating under isobaric conditions. The scheme of the setup is shown in Figure 2 and consists of a cylindrical sample chamber, with an inner volume of 9 mL, connected to a condenser area. A glassy-coil (Duran glass, Duran Group GmbH, Mainz, Germany), customized to fit the inner area of the condenser, is placed there to increase the surface area of the cooler and, thus, ensure an adequate cooling and reflux. The condenser module is connected by an adjustable connection (Rotulex 35/20, sealed by a Viton 500 O-ring) to a distribution rack, which consists of a Duran glass cylinder with four end-caps allowing for sealing or connection with two GL14 and two GL18

DOI: 10.1021/acs.jpcb.8b03278
J. Phys. Chem. B 2018, 122, 6017−6032

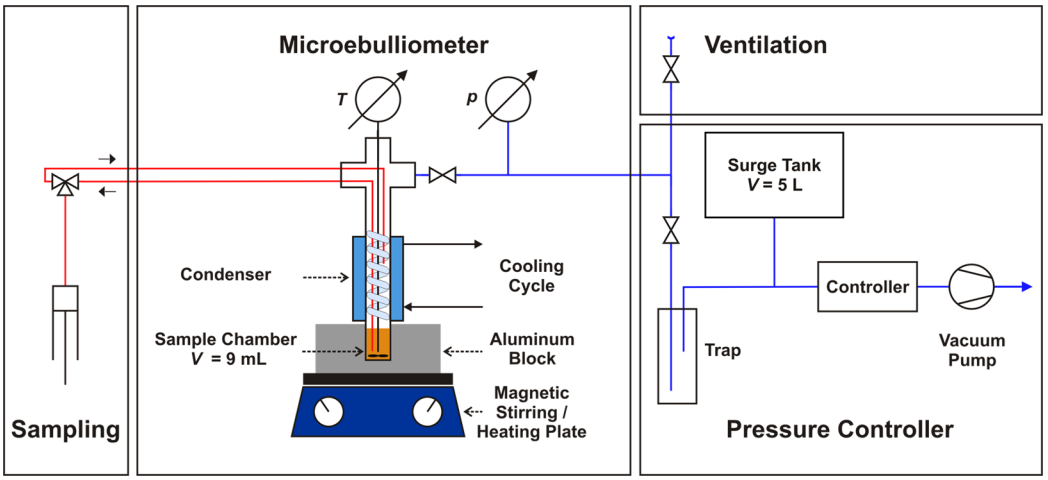

Figure 2. Sketch of the microebulliometer; the red lines symbolize the sample loop and the blue lines the vacuum line.

threads. The distribution rack connections allow connection of the ebulliometer to a vacuum line, a gastight tube for sampling, and placing a temperature sensor immersed in the mixture, through temperature resistant screw joints (Bola HT connection system; materials PFA, PPS, Bohlender GmbH, Grünsfeld, Germany). The connecting tube to the vacuum system has an inbuilt high-vacuum valve (orifice Ø: 0−10 mm, Gebr. Rettberg GmbH, Göttingen, Germany) to allow for a separation of the device from the vacuum-system. Inside the sample loop, PTFE and PFA hoses and a three way valve (valve HVX3-3, hoses and tubing system: Hamilton AG, Bonaduz, Switzerland) are integrated. They are connected with a syringe (Injekt-F V = 5 mL; B. Braun Melsungen AG, Melsungen, Germany) for sampling. The apparatus is heated by a block thermostat, regulated by a magnetic heating and stirring plate (type C-MAG HS7, IKA, Staufen, Germany), which also allows for stirring the liquid phase in the sample chamber. The block thermostat consists of an aluminum block (diameter: 150 mm; height: 50 mm) and was optimized to ensure stable conditions within a temperature range of 318 K < T < 423 K. The pressure level inside the entire setup is controlled by a vacuum system (PC 3003 Vario, Vacuubrand GmbH, Wertheim, Germany). In order to decrease fluctuations induced by the vacuum controller, a surge tank (type CRVZS-5, Festo AG, Esslingen, Germany) with a volume of 5 L is included within the vacuum line, ensuring pressure stability of $p = \pm$ 1.0 mbar.

In order to determine a VLE, the sample chamber is initially charged with a typical amount of 8 mL of the neat more volatile component (H_2O or C_nOH; n = 1−4, respectively). The boiling temperature of the neat component is then determined, allowing us to infer the adequate operational conditions. A temperature difference in between the aluminum block and the solvent's boiling temperature of typically ΔT = 15−30 K in combination with an adequate stirring of the sample leads to optimal boiling conditions and a permanent reflux. A small amount of the IL is then added to the sample and the system allowed to reach equilibrium. The formation of a saturated vapor phase can be monitored by the amount of reflux of the liquid inside the condenser and on the surface of the glassy coil. After typically t = 15−45 min, steady state conditions are achieved so that a continuous reflux is observed. If the composition of the sample is changed to mole fractions x(solvent) $\lesssim$ 0.4−0.6 only a dropwise reflux occurs. The pressure within the system is monitored by a pressure transducer (type P-30, Wika SE, Klingenberg, Germany) connected with a data acquisition unit (HP 34401A, Hewlett-Packard, Palo Alto, CA, USA) with an overall uncertainty of the device of $u(p) = \pm$ 1.4 mbar. The temperature of the boiling liquid is determined by a homemade glassy sealed Pt-100 sensor (cover Duran glass, Duran Group GmbH, Mainz, Germany; sensor: type 578-084, TC Mess- and Regeltechnik GmbH, Mönchengladbach, Germany) connected with a data acquisition unit (HP 34401A, Hewlett-Packard, Palo Alto, CA, USA) within an overall uncertainty of the temperature sensors of $u(T) = \pm$ 0.03 K (C_nOH series; n = 1, 3, 4) or $u(T) = \pm$ 0.06 K (water series and C_2OH series), respectively. Both the pressure and the temperature are monitored and logged by a computer based Labview script. Taking into account additional fluctuations in p and T monitored during an experiment, which are mainly due to the conditions of operation of the device and the conditions of stable boiling and reflux, uncertainties $u(T)$ and $u(p)$ are obtained, which are given together with the results in the Supporting Information in Tables S2−S8.

Sampling is performed by taking aliquots of typically 0.1 mL of the liquid phase and determining their index of refraction (Abbe refractometer type 51606, Carl Zeiss, Oberkochen, Germany). The composition of each sample is calculated using a predetermined calibration curve that, through error propagation, allows an accuracy of the solvent mole fraction of $u(x) = \pm$ 0.0004. The nature of the specific VLE phase behavior of highly asymmetric mixtures containing a component with negligible vapor pressure implies the assumption that the vapor phase is formed only by the more volatile component, that is the alcohol or water. In order to validate the alignment, the calibration and the assembly of the individual components prior to the characterization of each individual system, the temperature dependence of the vapor pressure of the neat solvents was monitored. Afterward, the composition of the mixture is changed stepwise by adding small aliquots of IL or even neat solvent to the sample inside the microebulliometer. By such systematic changes of the composition and the pressure conditions, respectively, the VLE is screened over a wide range of composition. At a certain composition, typically for alcohol mole fractions lower than $x(C_nOH)$ = 0.6, the viscous behavior of the mixture and the boiling conditions are hampering the formation of a steady state inside the apparatus. The reflux is reduced down to a randomly dropwise flow. Such conditions are an indication of the apparatus' detection limit and simultaneously explain the scatter

DOI: 10.1021/acs.jpcb.8b03278
J. Phys. Chem. B 2018, 122, 6017−6032

of the boiling temperatures and their uncertainties (cf. Tables S2−S8).

Soft-SAFT EoS Modeling. In order to describe the phase behavior of ILs by advanced models, the convoluted nature of these liquids has to be considered. ILs and several other associating components (e.g., water/alcohols), which are strongly influenced by strong and highly directional attractive forces (e.g., hydrogen bonding), disclose the known limitations of the traditional (and still standard[92]) cubic EoSs. Cubic EoSs exhibit a very limited accuracy when applied to the description of the thermodynamic properties and phase equilibria of such systems. This establishes the need for more robust and accurate models that are capable of taking these effects at the molecular level into account. One of the most promising routes arises from developing and applying molecular-based EoSs adapted from statistical thermodynamics principles. They explicitly account for different structural and energetic effects from the inception of the equation, providing a more realistic physical interpretation of the system. These equations allow isolating and quantifying the effects of the chain length, polarity, and hydrogen bond formation on the macroscopic properties of the system from explicitly considering information at the structural level. The first and utmost successful form of such an engineering EoS, SAFT (from Statistical Associating Fluid Theory), was first proposed by Chapman and co-workers in the late 80s.[93,94] In SAFT, a reference fluid (e.g., hard-sphere or Lennard-Jones) is perturbed by different contributions, each representing a specific effect to the fluids behavior, such as the nonspherical shape of molecules or the association phenomenon. Thus, SAFT-type EoSs are generally written as a sum of different terms to the residual Helmholtz energy, from which all the thermodynamic properties can then be easily derived. Different SAFT variants mainly differ on the reference term considered to model the physical interactions while using identical chain and association terms derived from Wertheim's perturbation theory.[95−98] Among them, soft-SAFT[86,87] is one of the most acknowledged due to its accuracy in describing a wide range of highly nonideal systems on the basis of a small amount of experimental data. Soft-SAFT has been successfully applied to several mixtures containing water,[99] ILs,[100−103] alcohols,[104] and their binary mixtures.[44,89]

In soft-SAFT,[86,87] the residual Helmholtz energy (A^{res}) for a n-component mixture of associating chain molecules is given as

$$A^{res} = A^{total} - A^{ideal} = A^{ref} + A^{chain} + A^{assoc} \tag{1}$$

where A^{ref} is the contribution due to the physical interactions in between the monomers or segments (groups of atoms assembling the molecule), A^{chain} is a term accounting for the chain formation from the individual segments, and A^{assoc} accounts for the short-range, strong, and highly directional forces such as hydrogen bonding, but in the case of the ILs also for the major energy contribution, the Coulombic interactions, between the charges of the cations and the anions.[105−109] The ion-charges are regarded as localized on the atoms so that the Coulomb contributions are described within the association framework. Thus, the long-range nature of the coulomb interactions is not explicitly considered. The soft-SAFT's reference term is given by a Lennard-Jones (LJ) spherical fluid considering both attractive and repulsive interactions in a single term as described by Johnson et al.[110] from molecular simulation data. A detailed description of the different terms can be found elsewhere.[86,87] Here, the reference term defines the LJ reference fluid using two molecular parameters: the spherical segment diameter of the monomers constituting the molecule, σ_{ii}, and the dispersive energy of interaction in between monomers, ε_{ii}/k_B. These two parameters along with the number of segments (i.e., the chain length), m_i, necessary in the chain term, characterize a nonassociating chain molecule within soft-SAFT. As the reference term was developed for a pure LJ fluid, the extension of soft-SAFT to mixtures is carried out by applying the van der Waals one-fluid theory coupled to the Lorentz−Berthelot mixing rules to obtain the unlike size and energy LJ parameters

$$\sigma_{ij} = \eta_{ij}\left(\frac{\sigma_i + \sigma_j}{2}\right) \tag{2}$$

$$\varepsilon_{ij} = \xi_{ij}\sqrt{\varepsilon_{ii}\varepsilon_{jj}} \tag{3}$$

In eqs 2 and 3, η_{ij} and ξ_{ij} are binary interaction parameters between the species i and j equivalent to the terms $(1 - l_{ij})$ and $(1 - k_{ij})$ used in classical cubic EoSs. They are adjusted by fitting when required to achieve a quantitative description of binary data and account for significant differences in the size and energy of the different monomers constituting the molecules present in the mixture. In a full predictive manner, both parameters are set to one, and mixture calculations are performed solely with the pure-component parameters. When dealing with associating molecules such as those investigated in this work, the association term, A^{assoc}, is enabled and square-well association sites considered to be embedded off-center in the core of some of the molecule's segments. The evaluation of this term requires two additional parameters: the bonding energy ($\varepsilon_{ii}^{HB}/k_B$) and the volume ($\kappa_{ii}^{HB}$) of the associating sites. If in the presence of more than one associating component, cross-association energies and volumes are given by the following mixing rules from the pure component parameters:

$$\varepsilon_{ij}^{HB} = \sqrt{\varepsilon_{ii}^{HB}\varepsilon_{jj}^{HB}} \tag{4}$$

$$\kappa_{ij}^{HB} = \left(\frac{\sqrt[3]{\kappa_{ii}^{HB}} + \sqrt[3]{\kappa_{jj}^{HB}}}{2}\right)^3 \tag{5}$$

Molecular Models. The reliability and accuracy of SAFT-type EoSs such as soft-SAFT rely on the proper selection of a coarse-grained model capable of representing most of the physical features of the compounds under study. This includes a proper fitting of the pure-component parameters (see the original work of Pàmies and Vega[111] and a more recent one by Oliveira et al.[112]) but also the specification of the number and type of association sites present in each molecule and the interactions allowed in the system (i.e., the association scheme). Such specification is usually carried out *a priori* based on the molecular structure of the molecules and/or quantum chemical calculations as data from NMR spectroscopy are usually unavailable. Methanol, ethanol, propan-1-ol, and butan-1-ol were previously investigated with soft-SAFT.[113,114] Alcohols were modeled as homonuclear chainlike molecules with the hydroxyl end-group being mimicked through two square-well association sites embedded off-center in one of the LJ segments (an (A) site mimicking the lone pair of electrons on the oxygen atom and a (B) site representing the H atom) with AB interactions being allowed for the pure component. Water is modeled, as proposed by Vega et al.,[115] using a 4-site associating model,[116] where two (C) sites are representing the H atoms and two (D) sites are mimicking the lone pairs of electrons in the oxygen atom and, similarly to the n - alkyl alcohols, CD

DOI: 10.1021/acs.jpcb.8b03278
J. Phys. Chem. B 2018, 122, 6017−6032

Table 1. Soft-SAFT Pure-Component Parameters Used within This Work

Compound	M_w/g/mol	m_i	σ_i/Å	ε_{ii}/k_B/K	ε^{HB}/k_B/K	κ^{HB}/Å^3	ref
methanol	32.04	1.491	3.375	220.4	3213	4847	113, 114
ethanol	46.07	1.740	3.635	234.8	3387	2641	113, 114
propan-1-ol	60.09	1.971	3.808	252.7	3450	2250	113, 114
butan-1-ol	74.12	2.210	3.940	269.2	3450	2250	113, 114
water	18.02	1.000	3.154	365.0	2388	2932	115
C_4mimTfO	288.29	4.149	4.375	378.0	3650	2400	89

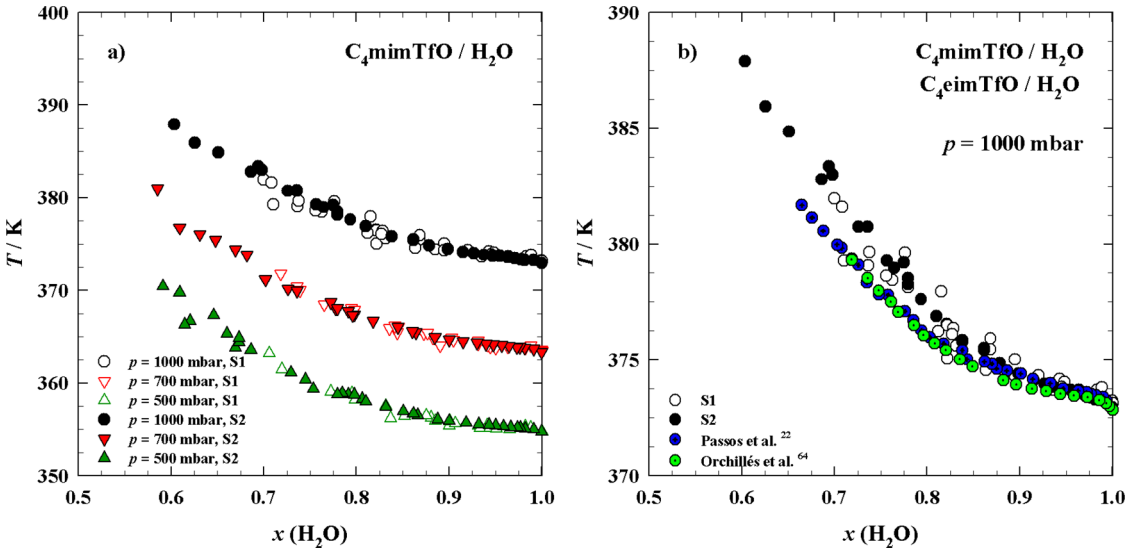

Figure 3. Isobaric VLE of the binary mixture of C_4mimTfO/H_2O: (a) obtained with the devices S1 and S2 at p = 500 mbar, 700 mbar, and 1000 mbar; (b) at p = 1000 mbar obtained with the devices S1 and S2 together with literature data from ref 22 and isobaric VLE data of the binary mixture C_4eimTfO/H_2O from ref 64.

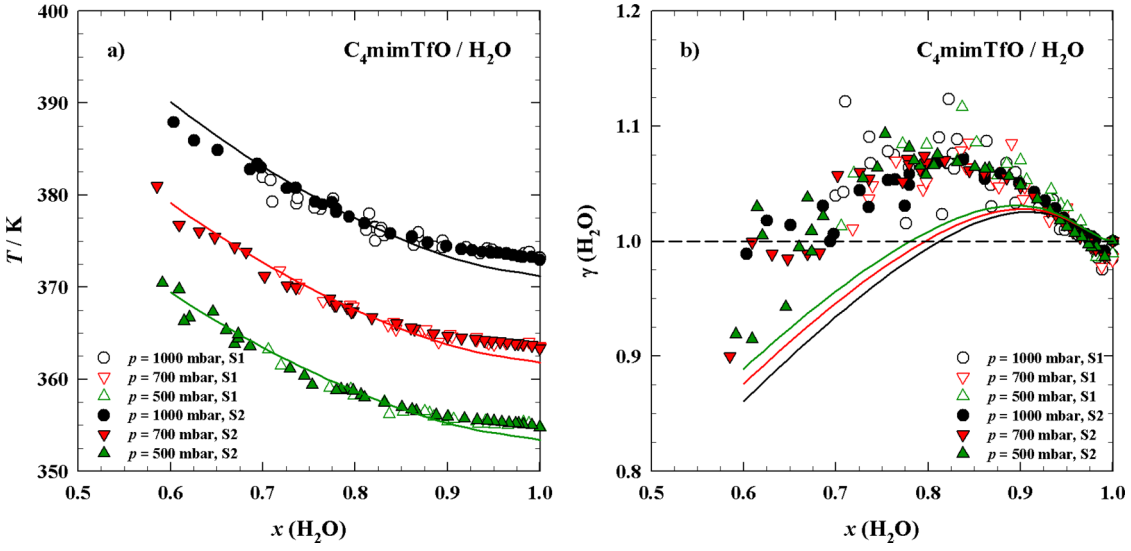

Figure 4. Isobaric VLE and activity coefficients of the binary mixture C_4mimTfO/H_2O. The solid lines represent the soft-SAFT EoS calculations.

interactions are allowed in pure water. Furthermore, Oliveira et al.[89] have considered C_4mimTfO to possess three associating sites: one association site (E) for the O^- interactions with the cation and two (F) sites to mimic the delocalized charge due to the presence of additional oxygen and fluorine atoms. Association between unlike sites was also allowed in the neat IL. When modeling the binary mixtures studied within this work, the cross-association interactions EB, ED, FA, and FC were taken into account as well. As molecular models and pure-component parameters were readily available from prior work for all the compounds under study, they are used here in a transferable manner and are reported in Table 1.

RESULTS AND DISCUSSION

Isobaric VLEs of the binary mixtures of C_4mimTfO and water or C_nOH (n = 1−4), respectively, were determined within this work applying three different pressure levels (p = 500 mbar, 700 mbar, and 1000 mbar). The requirements for reflux allow for a

DOI: 10.1021/acs.jpcb.8b03278
J. Phys. Chem. B 2018, 122, 6017−6032

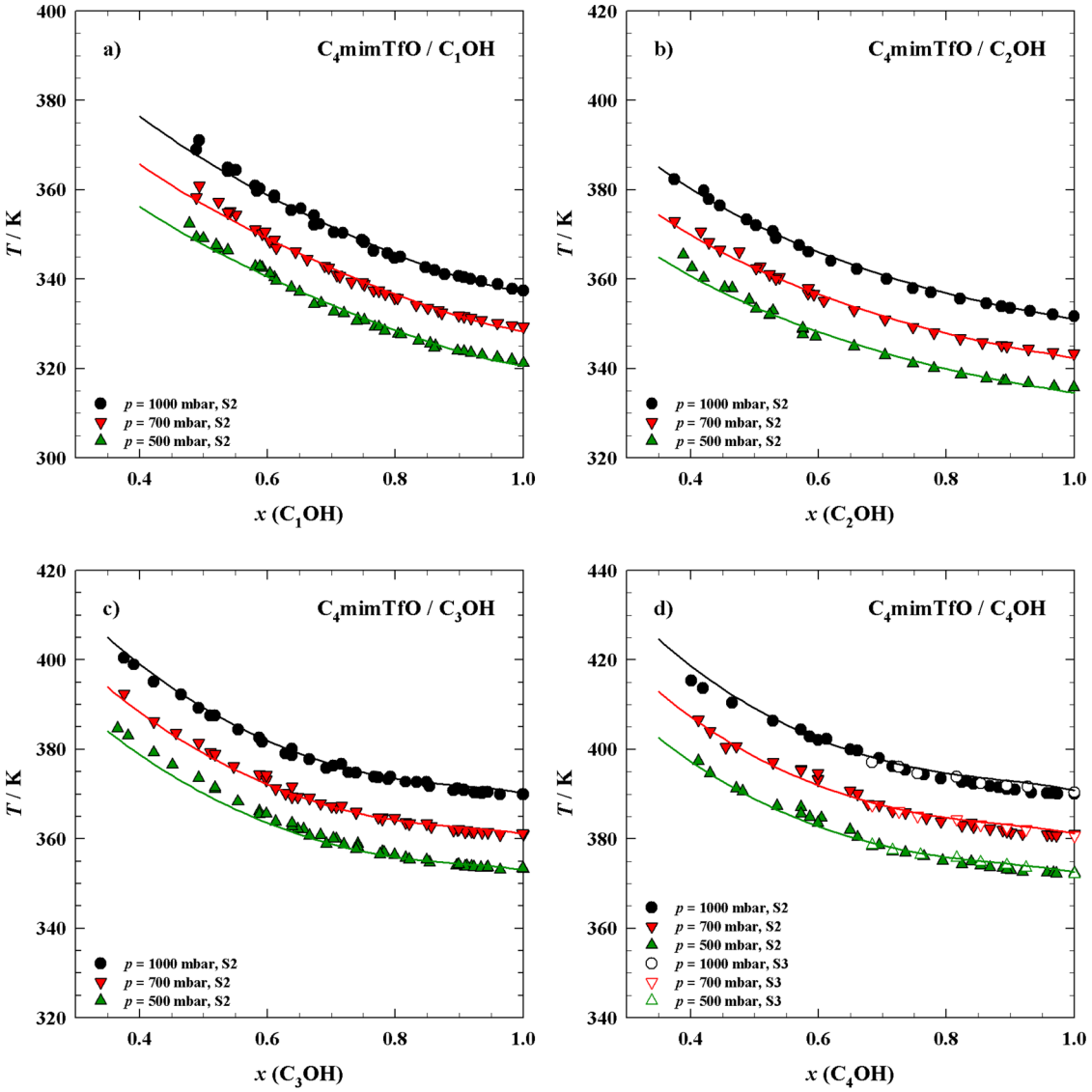

Figure 5. Isobaric VLEs of binary mixtures of C_4mimTfO/C_nOH (n = 1−4) obtained with the devices S2 and S3. The solid lines represent the corresponding soft-SAFT EoS calculations.

determination of the individual VLEs for mole fractions of the solvent in the range of 0.4−0.6 ≤ x(solvent) ≤ 1.0 and a temperature range of about 321.2 K ≤ T ≤ 415.4 K. These limits are clearly visible in the figures describing the results of the study (Figures 3−7) and are reported in Tables S2−S8. All the studied mixtures show deviations from an ideal behavior as illustrated by the activity coefficients represented in Figures 4b and 7, which are discussed in detail in a subsequent section of the manuscript.

Analysis of the Nonideal Behavior of the Binary Mixtures. In order to analyze the influence of the chemical structure of the solvent on the nonideal behavior of the mixtures, the activity coefficients γ_i of the volatile component i (water or C_nOH; n = 1−4) were calculated applying the modified Raoult's law:[117]

$$\gamma_i = \frac{y_i \cdot \varphi_i \cdot p}{x_i \cdot \varphi_i^{\sigma} \cdot p_i^{\sigma}} \tag{6}$$

where x_i and y_i are indicating the mole fraction of component i in the liquid and vapor phases, respectively, φ_i is indicating the fugacity coefficient of component i in the vapor phase, and φ_i^{σ} is indicating the fugacity coefficient of component i in its saturated state. The parameter p is the pressure of the system and p_i^{σ} is the vapor pressure of the pure component i at the system's temperature. The value of the ratio $\varphi_i/\varphi_i^{\sigma} \approx 1$ holds for the range of pressures and temperatures reached during the investigations.[117] Due to the insignificant low vapor pressure of the IL C_4mimTfO, it can be assumed that the vapor phase consists solely of the pure solvent. Hence, y_i is equal to one and eq 6 can be further simplified as

$$\gamma_i = \frac{p}{x_i \cdot p_i^{\sigma}} \tag{7}$$

The vapor pressure of the volatile components (water and the n-alkyl alcohols) in its equilibrium state, p_i^{σ}, is calculated by the following expression:

$$\ln p^{\sigma} = A + \frac{B}{T} + C \cdot \ln T + D \cdot T^{E} \tag{8}$$

The underlying data are obtained from the DIPPR database.[118] The values of the coefficients are listed in Table S1. In order to

DOI: 10.1021/acs.jpcb.8b03278
J. Phys. Chem. B 2018, 122, 6017−6032

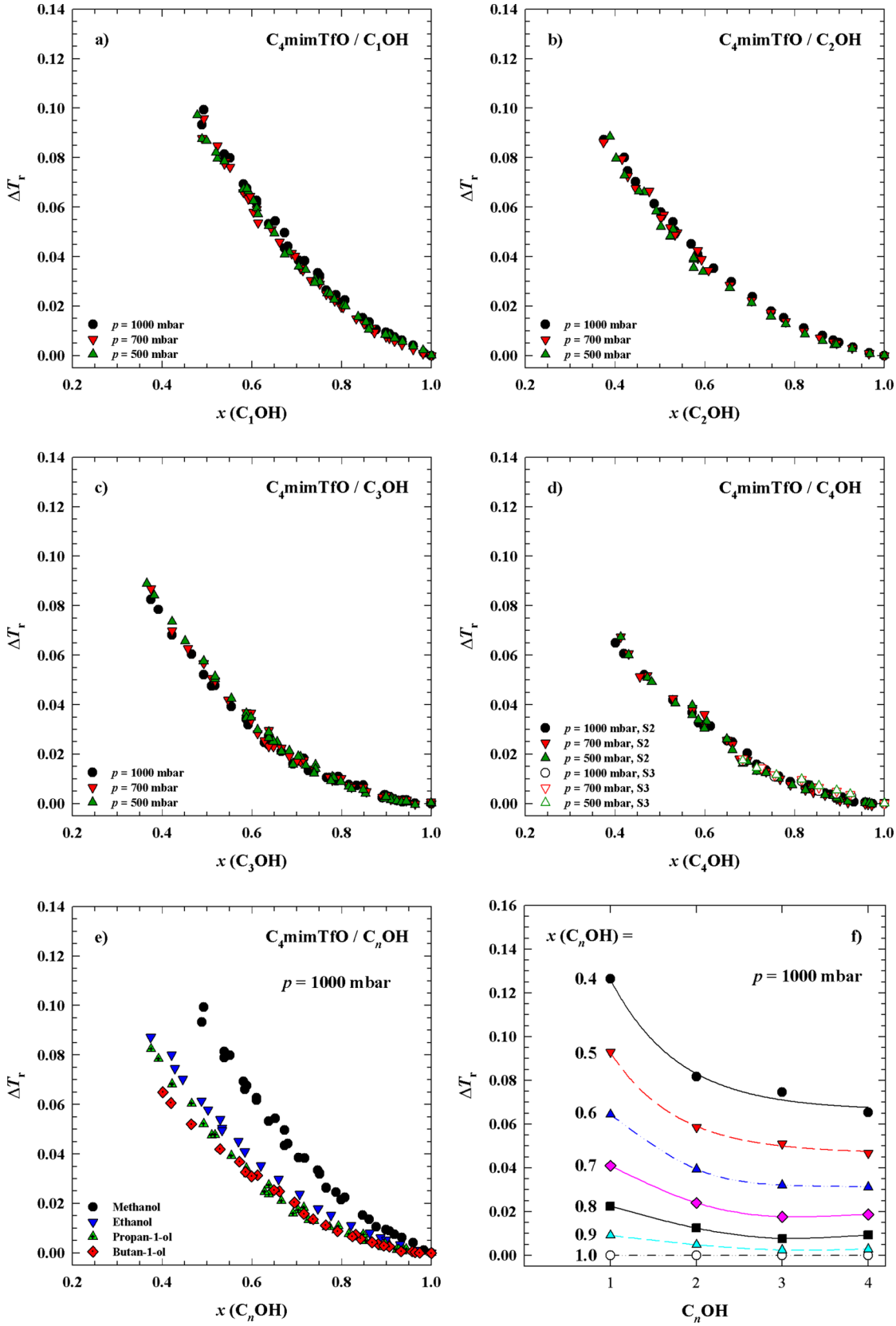

Figure 6. Normalized reduced deviations ΔT_r (cf. eq 10) of binary mixtures of C_4mimTfO/C_nOH (n = 1−4): (a) C_4mimTfO/C_1OH; (b) C_4mimTfO/C_2OH; (c) C_4mimTfO/C_3OH; (d) C_4mimTfO/C_4OH; (e) C_4mimTfO/C_nOH (n = 1−4) at p = 1000 mbar; (f) as a function of the chain length of the n-alkyl alcohol at selected constant mole fraction x(C_nOH) of the binary mixtures; lines are given to guide the eye.

validate the vapor pressure correlations and to allow for an assessment of experimental errors in accordance to ISO-GUM,[119] all of them were rechecked within the relevant temperature range and compared with experimental data

DOI: 10.1021/acs.jpcb.8b03278
J. Phys. Chem. B 2018, 122, 6017−6032

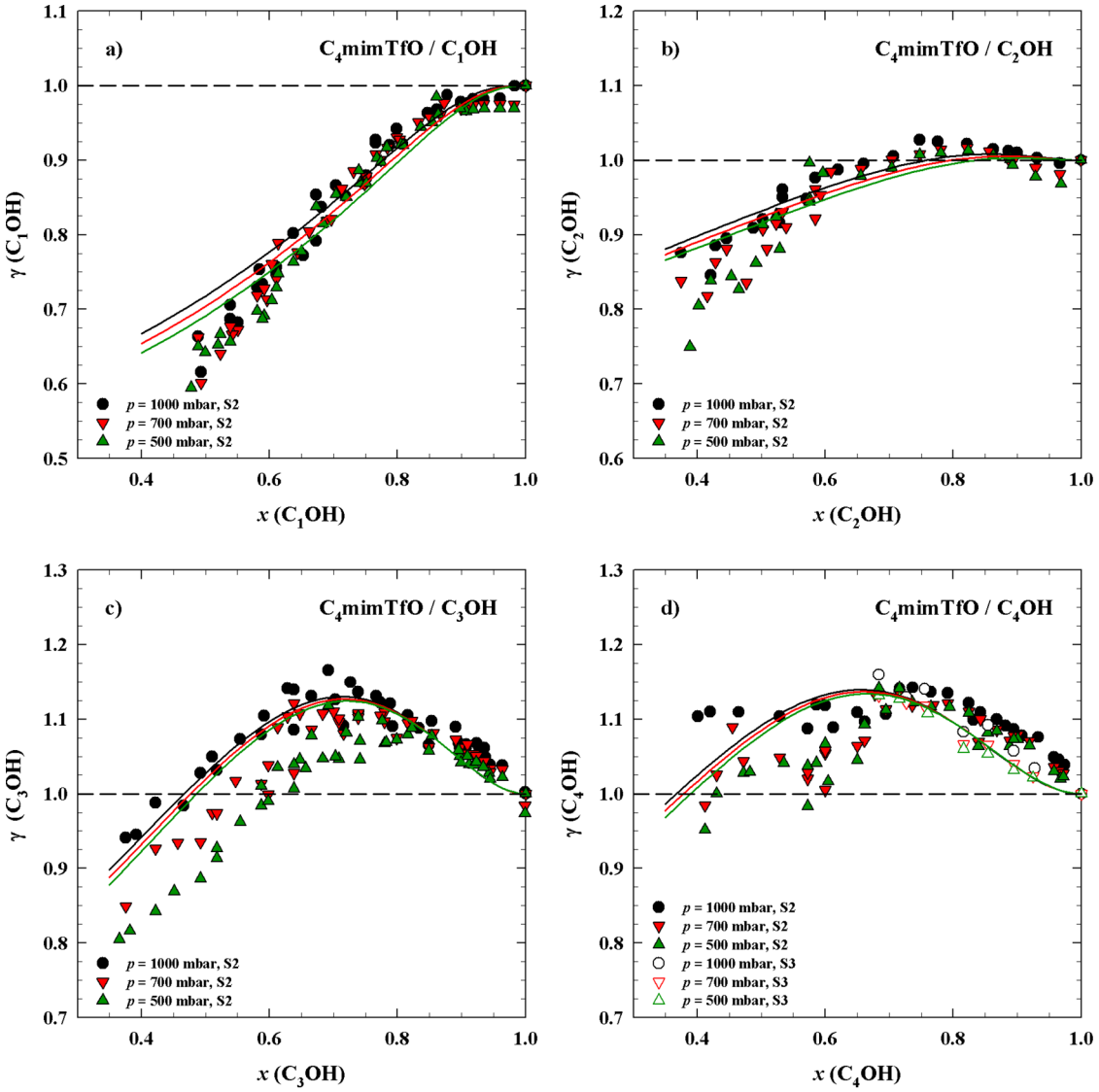

Figure 7. Activity coefficients as obtained by eq 7 of binary mixtures of C_4mimTfO/C_nOH (n = 1–4). The solid lines represent the soft-SAFT EoS descriptions.

published together with their uncertainty statements.[78,120−125] The uncertainty of the vapor pressures calculated by the DIPPR correlation is estimated by the maximum deviation between data from the literature and the DIPPR correlation and can be calculated by eq 9, where for practical reasons a correction coefficient u_c is introduced, which is also listed in Table S1:

$$\Delta p^{\sigma} = p^{\sigma} \cdot u_c \tag{9}$$

Results of 1-Butyl-3-methylimidazolium Trifluoromethanesulfonate/Water Mixtures. Beside the determination of the VLE of the mixture of C_4mimTfO and water, an interlaboratory test of individual but similarly designed set-ups, one in Aveiro (indicated as setup S1, described in Carvalho et al.[61]) and one in Bremen (indicated as setup S2, this work) has been carried out. The work aims at comparing the above-described VLE apparatus to a known, previously validated, VLE device[61] in order to verify the principle of operation and function. For this, binary mixtures of C_4mimTfO and H_2O were chosen as a reference system, since both components are completely miscible in the temperature range investigated.[126]

The isobaric VLE data of the mixtures of C_4mimTfO and H_2O are depicted in Figure 3 and are reported in Table S2 and Table S3.

As depicted in Figure 3, the VLEs were determined within a composition range of $0.6 \leq x(H_2O) \leq 1.0$ due to the limitation of the conditions for reflux.

Figure 3a shows the isobaric VLEs of the binary mixture C_4mimTfO/H_2O at pressures of p = 500 mbar, 700 mbar, and 1000 mbar obtained with the setup "S2". As shown there, an increase of the mole fraction of the IL in the binary mixture leads to an increase of the boiling temperature for all pressures. Furthermore, a decrease of the system pressure results in a decrease of the boiling point. Therefore, the three curves are shifted almost parallel along the temperature axis.

For the sake of comparison of the different set-ups S1 and S2, the binary VLEs determined with the devices S1 and S2 are both plotted in Figure 3a. The results map on each other within the experimental error; the data series obtained with setup S1 shows a slightly higher scatter. However, with both devices the boiling temperature of water as given in the DIPPR database[118] can be reproduced by 0.45 K, which is not visible on the scale of the

DOI: 10.1021/acs.jpcb.8b03278
J. Phys. Chem. B 2018, 122, 6017−6032

figure. A comparison of the VLEs to other data from the literature[22,64] is shown in Figure 3b. All data show a similar trend as those from Passos et al.;[22] however, the dependency of the boiling temperature on the mixture composition is more pronounced and shifted toward higher temperatures. The boiling temperatures obtained for a mole fraction of $x(H_2O) \approx 0.7$ are shifted up to $\Delta T \approx +1.6$ K in this work. Due to the lack of data from the literature, which may allow a critical assessment of the results, the VLE data of this work are also compared with data from Orchilles et al.[64] where a similar binary mixture of 1-butyl-3-ethylimidazolium trifluoromethanesulfonate and water (C_4eimTfO/H_2O) was investigated. Surprisingly, the data from refs 22 and 64 also map on each other and show the same deviation to the data determined within this work.

In order to analyze the interactions between the IL and the water molecules, the activity coefficients were calculated applying the modified Raoult's law (eq 7). Results are depicted in Figure 4 within the composition range of $0.6 \leq x(H_2O) \leq 1.0$.

The activity coefficients are illustrated in Figure 4b; the detailed data for each pressure are summarized in the Supporting Information (cf. Figure S1a–c). On the one hand, they indicate slightly positive deviations from Raoult's law ($\gamma_i > 1$) within most of the composition range covered in this study. On the other hand, they suggest that for more concentrated solutions the deviations would become negative. These deviations are a result of the weak interactions between the different molecular moieties, in particular the ionic liquid anion and the water molecules. The pressure dependency of the activity coefficient is insignificant within the pressure range investigated (cf. Figure 4b).

Results obtained by the different microebulliometers S1 and S2, indicated in the different plots by blank and filled symbols, respectively, are congruent as shown in Figure 3; systematic deviations are not visible. From this finding we conclude that both devices produce reliable VLE-data. As described in the following section additional effort was made to validate the microebulliometers against a classical VLE-setup (cf., the following section).

In order to classify the activity coefficients obtained within this work in the frame of literature results from refs 22 and 64, the activity coefficients obtained at a pressure of p = 1000 mbar are plotted together in Figure S1a. The values reported by Passos et al.[22] present a slightly higher positive deviation from unity compared to the data of the same mixture in the present study. The dependency of the data on the composition indicates a constant limit of $\gamma(H_2O) \approx 1.1$ for water compositions $x(H_2O) <$ 0.8 compared to the values of this work. The same behavior of the activity coefficients is described for the C_4eimTfO mixtures, calculated with data from ref 64 applying eq 7. This leads to the assumption that the length of the shorter alkyl side chain of the imidazolium-based cations has a minor effect on the molecular interactions and, thereby, on the resulting VLE.

The deviations of the activity coefficients of Passos et al.[22] and of the set-ups S1 and S2 are vanishing at pressures of p = 700 mbar and 500 mbar within the investigated composition range covered in this work, so that the curves map on each other (cf. Figure S1b and Figure S1c).

The accurate simulation and design of a refrigeration or absorption process requires the availability of accurate and robust thermodynamic models able to successfully describe the thermodynamic properties and phase behavior of the fluids involved. Therefore, and to grasp additional information about the molecular behavior of the mixtures under investigation, the experimental data were modeled using the soft-SAFT EoS. As reported in Table 2, one binary interaction parameter, ξ_{ij} = 1.13,

Table 2. Binary Interaction Parameters Used in the soft-SAFT Model and the Percentage Average Absolute Relative Deviation to the Experimental Boiling Temperatures

C_4mimTfO/solvent	η_{ij}	ξ_{ij}	%AARD(T/K)	%AARD(γ)
water		1.130	0.261	3.81
methanol		1.015	0.226	3.28
ethanol		0.985	0.186	2.55
propan-1-ol	0.950	0.980	0.210	3.11
butan-1-ol	0.950	0.980	0.281	3.41

correcting the mixtures dispersive energy, was required to achieve a quantitative agreement with the experimental data as shown in Figure 4. This parameter was found to be state independent and suggests the presence of higher unlike interactions in the mixture than those predicted by the combining rules considered from the pure component parameters. Moreover, although a good description of the experimental data was obtained in the entire composition range, the deviations to the experimental data systematically increase as the mole fraction of water is increased due to the known limitations of soft-SAFT when applied to describe pure water (e.g., the water boiling temperatures at the three different pressures are underpredicted by the soft-SAFT model). Nevertheless, as reported in Table 2, the values of percentage average absolute relative deviation (%AARD) are kept small in the whole range of experimental conditions.

The water activity coefficients in the liquid phase were also calculated with the soft-SAFT EoS from eq 1 as values for the fugacity coefficients and the vapor phase composition in equilibrium are readily available from the soft-SAFT framework. The results obtained from the model are compared with those estimated from the experimental data through eq 7 in Figure 4b. The results of the modeling validate the approximations made to simplify eq 1 to yield eq 2 as soft-SAFT estimates the molar fraction of the ionic liquid in the vapor phase to be lower than 1×10^{-5} in the experimental conditions and the ratio of the fugacity coefficients to be kept in the interval $1 \leq \varphi_i \leq 1.0016$. Therefore, the differences observed in Figure 4b between the activity coefficients obtained by soft-SAFT and those estimated from the experimental data are due to the different reference state considered for the water vapor pressure. As the vapor pressure calculated from soft-SAFT is lower than that obtained from the DIPPR correlation, the activity coefficients are systematically lower than the experimental values, predicting the shift from positive to negative deviations from the ideal behavior at a higher water concentration. The concentration dependence of activity coefficients of water reflects the breaking of the H-bond network by the ILs at high water concentration and the hydrogen bonding between water and the anions at higher IL concentrations. According to soft-SAFT and in agreement with the "experimental" activity coefficients, the pressure effect upon the alcohol–IL interactions seems to be negligible, although an increasing system pressure benefits the interactions between the two components.

Results of 1-Butyl-3-methylimidazolium Trifluoromethanesulfonate/*n*-Alkyl Alcohol Mixtures. Isobaric VLE data and the activity coefficients of the four binary mixtures C_4mimTfO/C_1OH, C_4mimTfO/C_2OH, C_4mimTfO/C_3OH, and C_4mimTfO/C_4OH at three different pressures (p = 500

DOI: 10.1021/acs.jpcb.8b03278
J. Phys. Chem. B 2018, 122, 6017–6032

mbar, 700 mbar, and 1000 mbar) were determined in this work. Experimental constraints allow for the determination of the VLE for mole fractions in the range of $0.4 \leq x(C_nOH) \leq 1.0$ to ensure a perfect (continuous) reflux inside the ebulliometer, which is a main requirement for reaching equilibrium conditions. Therefore, a temperature range of 321.2 K $\leq T \leq$ 415.4 K was covered.

To the best of our knowledge, there are no VLE data of those mixtures reported in the literature within the temperature, pressure, and composition ranges investigated here. In order to characterize the working range and the reproducibility of the microebulliometer, a second set of experiments on the VLE behavior for a selected system, C_4mimTfO/C_4OH, has been performed using a commercial VLE apparatus (Labo Dest Type 0600/II; Fischer Labor- and Verfahrenstechnik GmbH, Meckenheim, Germany; indicated as setup S3, this work). The experiments covered a composition range of $0.68 \leq x(C_4OH) \leq 1.0$. For mole fractions $0.68 < x(C_4OH)$ it was impossible to ensure stable boiling conditions resulting in an imperfect circulation inside the apparatus. This limit is indicated by a significant increase of scatter of the data obtained, and thus, the applicability of this type of apparatus is limited for these type of systems.

The isobaric VLE data of the binary IL/*n*-alkyl alcohol mixtures are depicted in Figure 5 and, together with error bars, in Figure S2; the data are given in Tables S4–S8.

Figures 5a–d show the isobaric VLEs of the binary mixtures C_4mimTfO/$C_{n=1,2,3,4}$OH obtained by the microebulliometer "S2". All the mixtures show similar trends, which are changing gradually and systematically. Decreasing the alcohol content in all mixtures results in an increase of the boiling temperature. This behavior is observed for the three pressure levels evaluated. By reduction of the system's pressure the boiling temperatures are shifted toward lower values. At first glance, the curves seem to be shifted parallel. In Figure 5d the experimental data obtained using the commercial device "S3" and that developed here, "S2", are compared. The data obtained from both apparatuses map perfectly on each other, giving clear evidence on the reliability of the data obtained. Unfortunately, the comparison for this data is limited by the narrow working range of the classical apparatus "S3". As mentioned above, the conditions for perfect circulation within the setup lead to this limit. In order to allow for an assessment of the data on a more general point of view, the general behavior of the single data sets has to be explained. Therefore, a relative shift of the temperature with respect to the boiling temperature of the neat alcohol $T_{0,b}$ is defined: $T_b - T_{0,b}$. Owing to the general concept of scaling in thermodynamics, this difference is normalized by $T_{0,b}$ to yield the following relative temperature deviation for each system studied in this work:

$$\Delta T_r = \frac{T_b - T_{0b}}{T_{0b}} \tag{10}$$

The normalized VLEs, the relative deviations ΔT_r of the mixture's boiling temperature to the neat solvent's boiling temperature of the mixture with alcohols, are depicted in Figures 6a–d.

Obviously, the behavior of the four mixtures is rather similar. In particular, all the different curves obtained at different pressures for each of the individual mixtures map on each other, which leads to the conclusion that the shape of the VLEs is independent of the system pressure within the investigated pressure, temperature, and composition range.

In order to analyze the effect of the alkyl chain length on the shape of the VLEs, the plots of the normalized reduced ΔT_r values calculated previously for the four investigated *n*-alkyl alcohols are combined in Figure 6e and 6f. Comparing the four curves in detail, the C_4mimTfO/C_1OH mixtures show a remarkably different behavior compared to the mixtures of the other alcohols. However, a small gradual shift between the single mixtures is visible; nevertheless, the cloud of data for C_2OH, C_3OH, and C_4OH show only narrow differences. From the experimental data, it may be speculated that the presence of secondary carbon atoms in the alcohol may play an important role in explaining the observed difference in between the methanol system and the mixtures with higher alcohols.

The soft-SAFT EoS was also applied to describe the VLEs of these four mixtures, and as shown in Figure 5, an excellent agreement with the experimental data was obtained with a maximum %AARD of 0.281 for the system C_4mimTfO/C_4OH. As reported in Table 2, a binary interaction parameter ξ_{ij}, very close to unity, correcting the energy of interaction between the two components was required. Its value approaches an asymptotic value of 0.98 as the alcohol's chain length is increased. Although this convergence for an asymptotic behavior on energy parameters when small structural changes of the components are being analyzed is common for SAFT-type equations, the study of longer chain alcohols would be required to further support this assumption. Additionally, for the mixtures with larger chain length alcohols, C_3OH and C_4OH, a size binary interaction parameter, that accounts for the size differences between the IL and the small alcohols LJ groups, was introduced in order to provide a quantitative agreement with the experimental data. Even though the use of such a parameter is often discouraged, huge size differences between the mixture components and their sparse sphericity may require their use. Moreover, different works show that it can be set to constant when modeling an homologous series of compounds and thus the value of η_{ij} was here fitted to the boiling temperatures of the mixture with propan-1-ol and successfully transferred to model the mixture with butan-1-ol. This kind of transferability of soft-SAFT parameters is one of the main advantages of SAFT-type equations. It is possible due to their strong theoretical background and the enhanced physical meaning of the different model parameters. The need for the size binary parameter is justified by the difference in size of the (LJ) groups making both components (the IL and the alkanols), as previously observed in several other asymmetric size systems. This parameter was not needed for methanol and ethanol because for these two compounds, the hydroxyl end-groups are the dominant interaction sites.

Similarly to what is observed in the experimental data, the curves obtained with soft-SAFT for the different system pressures are all shifted parallel along the temperature axis for all the four mixtures. Furthermore, the complex nature of the ionic liquid seems to be well represented by the molecular model considered in soft-SAFT, as the effect of increasing molar fractions of the ionic liquid in the mixture on the boiling temperatures is remarkably well captured by soft-SAFT reinforcing its reliability when applied to systems containing ILs.

Activity Coefficients of 1-Butyl-3-methylimidazolium Trifluoromethanesulfonate/*n*-Alkyl Alcohol Mixtures. In order to analyze the effect of the alkyl chain length on the VLE, and hence, molecular interactions and volatility, the activity coefficients of the mixtures were calculated applying eq 7. Results

DOI: 10.1021/acs.jpcb.8b03278
J. Phys. Chem. B 2018, 122, 6017–6032

are shown in Figure 7 and, more extensively including error bars, in Figure S3 and in Tables S4–S8.

From the results reported in Figure 6e a significant difference of the behavior of the various studied mixtures can be observed. This is corroborated by the activity coefficients depicted in Figure 7. For mixtures of C_4mimTfO/C_1OH (Figure 7a), negative deviations from Raoult's law ($\gamma(C_1OH) < 1$) are observed within the whole range of composition and pressure. The activity coefficients decrease with a decrease of C_1OH concentration in the binary mixture. A pressure dependence cannot be observed as the results of the different pressures map on each other.

The trends of the activity coefficients for the alcohol/IL system are rather similar to that observed for the water/IL systems, reflecting the breaking of the H-bond network by the ILs at high alcohol concentration and the hydrogen bonding between alcohol and the anions at higher IL concentrations.

However, varying the chain lengths of the alcohols, systematic changes of the behavior are found. As can be seen in Figure 7b for ethanolic mixtures, there is an evolution toward small but positive deviations from Raoult's law at $0.7 < x(C_2OH) < 1.0$. For $x(C_2OH) < 0.7$ the activity coefficients decrease with increasing IL-content. This behavior becomes more pronounced when considering C_3OH or C_4OH mixtures. Their activity coefficient curves show a behavior with a maximum around $x(C_nOH) \approx 0.66$, while the maximum for C_2OH is around $x(C_2OH) \approx 0.8$; a ratio of the molecular moieties of about 1:4.

In the composition range between $0.6 \leq x(C_2OH) \leq 1.0$ the three curves map on each other. However, a small pressure dependency can be observed for mole fractions $0.6 < x(C_2OH)$: a lower pressure leads to lower activity coefficients.

The activity coefficients of C_4mimTfO/C_3OH mixtures are shown in Figure 7c. Activity coefficients of $\gamma > 1$ are obtained for mole fractions of $0.6 \leq x(C_3OH) \leq 1.0$. The values of the activity coefficients increase with a decrease of the amount of C_3OH in the binary mixture, and a maximum is reached for a mole fraction of $x(C_3OH) \approx 0.66$, which is equal to a ratio of the molecular moieties of 2:1 (C_3OH:C_4mimTfO). A further decrease of the amount of C_3OH in the binary mixture results in a decrease of the activity coefficients. For mole fractions $x(C_3OH) < 0.5–0.6$ the values of the activity coefficients are $\gamma < 1$. Besides, the activity coefficients almost map on each other within the composition range of $0.8 \leq x(C_3OH) \leq 1$. The activity coefficients for mole fractions $x(C_3OH) < 0.8$ show a more pronounced pressure dependency.

An increase of the pressure of the system leads to a shift to higher activity coefficients. However, the data at $p = 700$ mbar maps on the other two curves within the error bars. The activity coefficients at $p = 1000$ mbar and $p = 500$ mbar do not map at those mole fractions.

In Figure 7d the activity coefficients of C_4mimTfO/C_4OH mixtures are depicted. They were determined with the devices S2 and S3. Activity coefficients of $\gamma > 1$ were obtained within the complete range of mole fractions of $0.4 \leq x(C_4OH) \leq 1.0$ covered in this work. A decrease of the amount of C_4OH results in an increase of the activity coefficients up to mole fractions of about $x(C_4OH) \approx 0.66$, which is equal to a 2:1 ratio of the different molecular moieties C_4OH and C_4mimTfO. The behavior retraces the findings drawn in Figure 7. A further decrease of the mole fraction of C_4OH leads to constant activity coefficients of $\gamma(C_4OH) \approx 1.1$ at $p = 1000$ mbar; at the pressure levels of $p = 500$ mbar and $p = 700$ mbar, the activity coefficients decrease and fluctuate around $\gamma(C_4OH) \approx 1$. However, they map on each other within their error bars in the investigated range. Due to the scatter of the data no clear dependency on the pressure can be extracted (cf. Figure S3d).

In order to assess the effect of the length of the *n*-alkyl chain of the different alcohols on the molecular interplay within the solutions, the activity coefficients have to be considered. Activity coefficients $\gamma < 1$ indicate a negative deviation from Raoult's law, which arises from favored interactions between the alcohol and the IL moieties. The interactions in between similar moieties, namely alcohol–alcohol and C_4mimTfO–C_4mimTfO molecules are somewhat weaker. Thus, the alcohol remains in the liquid phase, indicating a depression of the vapor pressure. On the other hand, activity coefficients $\gamma > 1$ indicate positive deviations from Raoult's law. In that case the interactions between similar moieties are favored compared to the interactions between the alcohol and the IL moieties, which results in an overall increase of the volatility.

The molecular interactions between the C_4mimTfO and the *n*-alkyl alcohols decrease with an increase of the chain length of the alcohols resulting in a stronger increase of the relative boiling temperatures (cf. Figure 7). The weakest interactions between the C_4mimTfO and the *n*-alkyl alcohol C_3OH and C_4OH moieties were observed in this work at mole fractions of about $x(C_nOH) \approx 0.66$ ($n = 3, 4$).

The alcohol activity coefficients were calculated with soft-SAFT from eq 1 and, as previously observed for the water activity coefficients in the system C_4mimTfO/H_2O, the assumptions behind eq 2, used to obtain the experimental activity coefficients, were found to remain valid as the influence of both the ratio of fugacities and the ionic liquid molar fraction in the vapor phase are negligible. The activity coefficients obtained with soft-SAFT are plotted against those estimated from the mixture boiling temperatures in Figure 7. A good agreement is observed with lower %AARD values (Table 2) than those previously observed in the mixture with water. This is due to the better description of the neat *n*-alkyl alcohols when compared to that of pure water.

As depicted in Figure 7, soft-SAFT is able to correctly capture the trends observed experimentally on the alcohols activity coefficients: In the binary mixture C_4mimTfO/C_1OH, negative deviations from the ideal behavior are observed in the whole composition range with the alcohols activity coefficients decreasing as the mixture becomes richer in ionic liquid. However, for ionic liquid mole fractions higher than 0.5, the model predicts a much weaker dependence of the activity coefficients on composition than that suggested by the experimental data points. As the alkyl chain length of the alcohols is increased, the model predicts a decrease on the IL–alcohol interactions and, thus, negative deviations from the ideal behavior. In fact, near the full solvation regime region (high alcohol concentrations), positive deviations to the ideal behavior and a positive maximum of the alcohol activity coefficients are observed. The dimension of this region, where positive deviations to the ideal behavior exist, and the value of the mentioned maximum clearly increase as the alcohols chain length is increased.

Moreover, although the pressure effect is not observed experimentally (especially for methanol and ethanol), the model suggests that contrarily to what is observed in the mixture with water, a minor negative effect is shown upon the magnitude of the IL–alcohol interactions as the activity coefficients increase with pressure. Nevertheless, according to the model the pressure effect fades as the alcohols chain length increases.

DOI: 10.1021/acs.jpcb.8b03278
J. Phys. Chem. B 2018, 122, 6017–6032

Comparison to Other Works. A detailed study focused on the structural effects of alcohols (*n*-alkyl alcohols, secondary, and tertiary ones), and the IL 1-butyl-3-methylimidazolium chloride (C_4mimCl) on the VLE is reported in Chouireb et al.[44] The data of their work and this work show the same trends and a systematic similar behavior. A decrease of the alcohol content in all binary mixtures results in an increase of boiling temperatures, which is observed for the three pressure levels investigated. By reducing the pressure, the boiling temperatures are shifted toward lower values. Besides, normalizing the VLEs of Chouireb et al. by eq 10 results in a similar picture as observed in this work. All different curves obtained at different pressure levels for each of the single mixtures map on each other. This supports the assumption that the shape of the VLEs is independent of the system pressure within the investigated pressure, temperature, and composition ranges.

Furthermore, a similar trend of the activity coefficients can be observed in both studies. Decreasing the alkyl chain length of the alcohol results in a decrease of the activity coefficients. Nevertheless, all C_4mimCl mixtures from the literature[44] show activity coefficients $\gamma < 1$ within the pressure, temperature, and composition ranges compared to the C_4mimTfO/C_nOH (n = 3, 4) mixtures, where activity coefficients of $\gamma > 1$ within a composition range $0.6 \leq x(C_4OH) \leq 1.0$ are determined. This leads to the conclusion that the molecular interactions between the IL C_4mimCl and the alcohol moieties are stronger than the molecular interactions between like IL-IL and alcohol−alcohol moieties. In turn, this allows us to conclude that the molecular interactions in the C_4mimCl mixtures are stronger than the molecular interactions in the C_4mimTfO mixtures.

CONCLUSIONS

VLEs of five binary mixtures of C_4mimTfO with water or an *n*-alkyl alcohol ($C_{n=1,2,3,4}OH$) obtained by isobaric ebulliometry were reported within this work. The study was conducted at three different pressure levels, p = 500, 700, and 1000 mbar. The boiling temperatures of the mixtures were found to increase with an increase of the ionic liquid concentration while a decrease of the pressure shifts the VLE toward lower boiling temperatures. The scatter of the data was low and its good accuracy allowed for a discussion of the different data sets and a further assessment of their nonideal behavior. By scaling the different boiling curves, it became evident that the general shape of the VLEs is not strongly dependent on the system's pressure, within the studied range.

The results of the activity coefficients show that a decrease of the alkyl chain length of the alcohol induces stronger interactions between the IL and alcohol moieties resulting in negative deviations from Raoult's law ($\gamma < 1$).

Results of some data sets were cross checked with different microebulliometers and, for C_4OH, with a classical VLE apparatus. The results obtained support the congruency and consistency of the data, regardless of the device used for the measurements.

Furthermore, the soft-SAFT EoS was used to describe the experimental data using coarse-grained models previously proposed for both the ionic liquid and the molecular solvents. By using one or, in some cases, two binary interaction parameters, temperature, composition, and pressure independent, a simultaneous accurate description of the mixture boiling temperatures and the water/alcohol activity coefficients was achieved. The simple models used in soft-SAFT, where the components are represented as associating chain-like molecules, provided an overall good description of the studied mixtures with an %AARD lower than 0.3% and 3.9% for the VLE and activity coefficients, respectively. Moreover, the information gauged from the modeling contributed to a deeper discussion of the different effects upon the IL−solvent interactions such as temperature, pressure, composition, and solvent's chemical structure. The results obtained reinforce the soft-SAFT EoS as a valuable tool for the description of mixtures containing ionic liquids, providing vital information for the design and implementation of new refrigeration systems.

ASSOCIATED CONTENT

Supporting Information

The Supporting Information is available free of charge on the ACS Publications website at DOI: 10.1021/acs.jpcb.8b03278.

Figure S1, activity coefficients of the binary mixture C_4mimTfO/H_2O; Figure S2, isobaric VLEs of binary mixtures of C_4mimTfO/C_nOH (n = 1, 2, 3, 4) with error bars; Figure S3, their corresponding activity coefficients with error bars; Table S1, coefficients used in eq 8 for calculation of solvent vapor pressures; Table S2−S8, comprehensive lists of VLE data of the mixtures C_4mimTfO/H_2O and C_4mimTfO/C_nOH (n = 1, 2, 3, 4) including uncertainties (PDF)

AUTHOR INFORMATION

Corresponding Author

*Tel.: +49 421 218 64772; fax: +49 421 218 64771; e-mail: rathke@uni-bremen.de.

ORCID

Pedro J. Carvalho: 0000-0002-1943-0006
João A. P. Coutinho: 0000-0002-3841-743X
Johannes Kiefer: 0000-0002-0837-3456
Bernd Rathke: 0000-0002-3333-1960

Notes

The authors declare no competing financial interest.

ACKNOWLEDGMENTS

The authors gratefully acknowledge financial support by Forschungsförderung Universität Bremen and by the STSM of M. Stuckenholz within the COST action CM1206-30741, EXIL - Exchange on Ionic Liquids. This work was developed in the scope of the project CICECO-Aveiro Institute of Materials, POCI-01-0145-FEDER-007679 (ref. FCT UID/CTM/50011/2013), funded by FEDER through COMPETE2020 - Programa Operacional Competitividade e Internacionalização (POCI) and by national funds through FCT -Fundação para a Ciência e a Tecnologia. P. J. Carvalho acknowledges FCT for a contract under the Investigador FCT 2015, Contract IF/00758/2015, and E. A. Crespo acknowledges Ph.D. Grant SFRH/BD/130870/2017.

REFERENCES

(1) Smolen, S.; Budnik-Rodz, M. Low Rate Energy Use For Heating and in Industrial Energy Supply Systems - Some Technical and Economical Aspects. *Energy* **2006**, *31*, 2588−2603.

(2) Horuz, I.; Kurt, B. Absorption Heat Transformers and an Industrial Application. *Renewable Energy* **2010**, *35*, 2175−2181.

(3) Sun, J.; Fu, L.; Zhang, S. G. A Review of Working Fluids of Absorption Cycles. *Renewable Sustainable Energy Rev.* **2012**, *16*, 1899−1906.

DOI: 10.1021/acs.jpcb.8b03278
J. Phys. Chem. B 2018, 122, 6017−6032

(4) Khamooshi, M.; Parham, K.; Atikol, U. Overview of Ionic Liquids Used as Working Fluids in Absorption Cycles. *Adv. Mech. Eng.* **2013**, *5*, 620592.
(5) Wu, W.; Zhang, H. Y.; You, T.; Li, X. T. Performance Comparison of Absorption Heating Cycles Using Various Low-GWP and Natural Refrigerants. *Int. J. Refrig.* **2017**, *82*, 56−70.
(6) Zheng, D. X.; Dong, L.; Huang, W. J.; Wu, X. H.; Nie, N. A Review of Imidazolium Ionic Liquids Research and Development Towards Working Pair of Absorption Cycle. *Renewable Sustainable Energy Rev.* **2014**, *37*, 47−68.
(7) Sun, J. A.; Fu, L.; Zhang, S. G. Performance Calculation of Single Effect Absorption Heat Pump Using LiBr + LiNO3 + H2O as Working Fluid. *Appl. Therm. Eng.* **2010**, *30*, 2680−2684.
(8) Kim, K. S.; Shin, B. K.; Lee, H.; Ziegler, F. Refractive Index and Heat Capacity of 1-Butyl-3-methylimidazolium Bromide and 1-Butyl-3-methylimidazolium Tetrafluoroborate, and Vapor Pressure of Binary Systems for 1-Butyl-3-methylimidazolium Bromide Plus Trifluoroethanol and 1-Butyl-3-methylimidazolium Tetrafluoroborate Plus Trifluoroethanol. *Fluid Phase Equilib.* **2004**, *218*, 215−220.
(9) Abumandour, E.-S.; Mutelet, F.; Alonso, D. Are Ionic Liquids Suitable as New Components in Working Mixtures for Absorption Heat Transformers ? In *Progress and Developments in Ionic Liquids*; Handy, S., Ed.; InTech: 2017.
(10) Ziegler, F. Recent Developments and Future Prospects of Sorption Heat Pump Systems. *Int. J. Therm. Sci.* **1999**, *38*, 191−208.
(11) Wu, W.; Wang, B. L.; Shi, W. X.; Li, X. T. An Overview of Ammonia-Based Absorption Chillers and Heat Pumps. *Renewable Sustainable Energy Rev.* **2014**, *31*, 681−707.
(12) Kob, N. E. Dibasic Ester: A Low Risk, Green Organic Sovent Alternative. In *Clean Solvents - Alternative Media for Chemical Reactions and Processing*; Abraham, M. A.; Moens, L., Eds.; American Chemical Society: Washington, D.C., 2002; pp 238−241.
(13) Plechkova, N. V.; Seddon, K. R. Applications of Ionic Liquids in the Chemical Industry. *Chem. Soc. Rev.* **2008**, *37*, 123−150.
(14) Anastas, P.; Eghbali, N. Green Chemistry: Principles and Practice. *Chem. Soc. Rev.* **2010**, *39*, 301−312.
(15) Sheldon, R. A. Fundamentals of Green Chemistry: Efficiency in Reaction Design. *Chem. Soc. Rev.* **2012**, *41*, 1437−1451.
(16) Werner, S.; Haumann, M.; Wasserscheid, P. Ionic Liquids in Chemical Engineering. In *Annual Review of Chemical and Biomolecular Engineering, Vol 1*; Prausnitz, J. D. M. F.; Segalman, R. A., Ed.; Annual Reviews: Palo Alto, 2010; Vol. *1*, pp 203−230.
(17) Heintz, A. Recent Developments in Thermodynamics and Thermophysics of Non-Aqueous Mixtures Containing Ionic Liquids. A Review. *J. Chem. Thermodyn.* **2005**, *37*, 525−535.
(18) Holbrey, J. D.; Rogers, R. D. Physicochemical Properties of Ionic Liquids: Melting Points and Phase Diagrams. In *Ionic Liquids in Synthesis*, 2nd, completely rev. and enl. ed ed.; Wasserscheid, P., Welton, T., Eds.; Wiley-VCH: Weinheim, 2008.
(19) Marsh, K. N.; Boxall, J. A.; Lichtenthaler, R. Room Temperature Ionic Liquids and Their Mixtures - A Review. *Fluid Phase Equilib.* **2004**, *219*, 93−98.
(20) Wasserscheid, P.; Welton, T. *Ionic Liquids in Synthesis*. In 2nd, completely rev. and enl. ed ed.; Wiley-VCH: Weinheim, 2008.
(21) Pereiro, A. B.; Araujo, J. M. M.; Esperanca, J. M. M. S.; Marrucho, I. M.; Rebelo, L. P. N. Ionic liquids in Separations of Azeotropic Systems - A Review. *J. Chem. Thermodyn.* **2012**, *46*, 2−28.
(22) Passos, H.; Khan, I.; Mutelet, F.; Oliveira, M. B.; Carvalho, P. J.; Santos, L. M. N. B. F.; Held, C.; Sadowski, G.; Freire, M. G.; Coutinho, J. A. P. Vapor-Liquid Equilibria of Water Plus Alkylimidazolium-Based Ionic Liquids: Measurements and Perturbed-Chain Statistical Associating Fluid Theory Modeling. *Ind. Eng. Chem. Res.* **2014**, *53*, 3737−3748.
(23) Seddon, K. R.; Stark, A.; Torres, M. J. Influence of Chloride, Water, and Organic Solvents on the Physical Properties of Ionic Liquids. *Pure Appl. Chem.* **2000**, *72*, 2275−2287.
(24) Romich, C. H.; Merkel, N.; Schaber, K.; Schubert, T.; Koch, M. Int Inst, R., A Comprarison Between Lithiumbromide - Water and Ionic Liquid - Water as Working Solution for Absorption Refrigeration Cycles. In *23rd Iir International Congress of Refrigeration*; Int Inst Refrigeration: Paris, 2011; *23*, 941−948.
(25) Romich, C.; Merkel, N. C.; Valbonesi, A.; Schaber, K.; Sauer, S.; Schubert, T. J. S. Thermodynamic Properties of Binary Mixtures of Water and Room-Temperature Ionic Liquids: Vapor Pressures, Heat Capacities, Densities, and Viscosities of Water Plus 1-Ethyl-3-methylimidazolium Acetate and Water plus Diethylmethylammonium Methane Sulfonate. *J. Chem. Eng. Data* **2012**, *57*, 2258−2264.
(26) Merkel, N. C.; Romich, C.; Bernewitz, R.; Kunemund, H.; Gleiss, M.; Sauer, S.; Schubert, T. J. S.; Guthausen, G.; Schaber, K. Thermophysical Properties of the Binary Mixture of Water Plus Diethylmethylammonium Trifluoromethanesulfonate and the Ternary Mixture of Water Plus Diethylmethylammonium Trifluoromethanesulfonate Plus Diethylmethylammonium Methanesulfonate. *J. Chem. Eng. Data* **2014**, *59*, 560−570.
(27) Merkel, N.; Weber, C.; Faust, M.; Schaber, K. Influence of Anion and Cation on the Vapor Pressure of Binary Mixtures of Water Plus Ionic Liquid and on the Thermal Stability of the Ionic Liquid. *Fluid Phase Equilib.* **2015**, *394*, 29−37.
(28) Yokozeki, A.; Shiflett, M. B. Water Solubility in Ionic Liquids and Application to Absorption Cycles. *Ind. Eng. Chem. Res.* **2010**, *49*, 9496−9503.
(29) He, Z. B.; Zhao, Z. C.; Zhang, X. D.; Feng, H. Thermodynamic Properties of New Heat Pump Working Pairs: 1,3-Dimethylimidazolium Dimethylphosphate and Water, Ethanol and Methanol. *Fluid Phase Equilib.* **2010**, *298*, 83−91.
(30) Yokozeki, A.; Shiflett, M. B. Vapor-Liquid Equilibria of Ammonia Plus Ionic Liquid Mixtures. *Appl. Energy* **2007**, *84*, 1258−1273.
(31) Sun, G. M.; Huang, W. J.; Zheng, D. X.; Dong, L.; Wu, X. H. Vapor-Liquid Equilibrium Prediction of Ammonia-Ionic Liquid Working Pairs of Absorption Cycle Using UNIFAC Model. *Chin. J. Chem. Eng.* **2014**, *22*, 72−78.
(32) Kerle, D.; Ludwig, R.; Geiger, A.; Paschek, D. Temperature Dependence of the Solubility of Carbon Dioxide in Imidazolium-Based Ionic Liquids. *J. Phys. Chem. B* **2009**, *113*, 12727−12735.
(33) Kerle, D.; Jorabchi, M. N.; Ludwig, R.; Wohlrab, S.; Paschek, D. A Simple Guiding Principle for the Temperature Dependence of the Solubility of Light Gases in Imidazolium-Based Ionic Liquids Derived from Molecular Simulations. *Phys. Chem. Chem. Phys.* **2017**, *19*, 1770−1780.
(34) Shiflett, M. B.; Yokozeki, A. Solubilities and Diffusivities of Carbon Dioxide in Ionic Liquids: [Bmim][PF6] and [Bmim][BF4]. *Ind. Eng. Chem. Res.* **2005**, *44*, 4453−4464.
(35) Shiflett, M. B.; Kasprzak, D. J.; Junk, C. P.; Yokozeki, A. Phase Behavior of {Carbon Dioxide Plus [Bmim][Ac]} Mixtures. *J. Chem. Thermodyn.* **2008**, *40*, 25−31.
(36) Shiflett, M. B.; Yokozeki, A. Phase Behavior of Carbon Dioxide in Ionic Liquids: [Emim][Acetate], [Emim][Trifluoroacetate], and [Emim][Acetate] Plus [Emim][Trifluoroacetate] Mixtures. *J. Chem. Eng. Data* **2009**, *54*, 108−114.
(37) Mondal, B. K.; Bandyopadhyay, S. S.; Samanta, A. N. Equilibrium Solubility and Enthalpy of CO2 Absorption in Aqueous Bis (3-Aminopropyl) Amine and its Mixture with MEA, MDEA, AMP and K2CO3. *Chem. Eng. Sci.* **2017**, *170*, 58−67.
(38) Shiflett, M. B.; Niehaus, A. M. S.; Yokozeki, A. Separation of N2O and CO2 Using Room-Temperature Ionic Liquid [Bmim][BF4]. *J. Phys. Chem. B* **2011**, *115*, 3478−3487.
(39) Kim, S.; Kim, Y. J.; Joshi, Y. K.; Fedorov, A. G.; Kohl, P. A. Absorption Heat Pump/Refrigeration System Utilizing Ionic Liquid and Hydrofluorocarbon Refrigerants. *J. Electron. Packag.* **2012**, *134* (031009), 1−9.
(40) Kim, S.; Kohl, P. A. Theoretical and Experimental Investigation of an Absorption Refrigeration System Using R134/[Bmim][PF6] Working Fluid. *Ind. Eng. Chem. Res.* **2013**, *52*, 13459−13465.
(41) Kim, S.; Patel, N.; Kohl, P. A. Performance Simulation of Ionic Liquid and Hydrofluorocarbon Working Fluids for an Absorption Refrigeration System. *Ind. Eng. Chem. Res.* **2013**, *52*, 6329−6335.

DOI: 10.1021/acs.jpcb.8b03278
J. Phys. Chem. B 2018, 122, 6017−6032

(42) Ren, W.; Scurto, A. M. Phase Equilibria of Imidazolium Ionic Liquids and the Refrigerant Gas, 1,1,1,2-Tetrafluoroethane (R-134a). *Fluid Phase Equilib.* **2009**, *286*, 1−7.
(43) Massel, M.; Revelli, A. L.; Paharik, E.; Rauh, M.; Mark, L. O.; Brennecke, J. F. Phase Equilibrium, Excess Enthalpies, and Densities of Binary Mixtures of Trimethylbutylammonium Bis-(trifluoromethylsulfonyl)imide with Ethanol, 1-Propanol, and Dimethylformamide. *J. Chem. Eng. Data* **2015**, *60*, 65−73.
(44) Chouireb, N.; Khan, I.; Crespo, E. A.; Oliveira, M. B.; Llovell, F.; Vega, L. F.; Tafat-Igoudjilene, O.; Kaci, A. A.; Santos, L. M. N. B. F.; Carvalho, P. J.; et al. Evaluation of the Solvent Structural Effect Upon the Vapor - Liquid Equilibrium of [C(4)C(1)im][Cl] + Alcohols. *Fluid Phase Equilib.* **2017**, *440*, 36−44.
(45) Khan, I.; Batista, M. L. S.; Carvalho, P. J.; Santos, L. M. N. B. F.; Gomes, J. R. B.; Coutinho, J. A. P. Vapor-Liquid Equilibria of Imidazolium Ionic Liquids with Cyano Containing Anions with Water and Ethanol. *J. Phys. Chem. B* **2015**, *119*, 10287−10303.
(46) Orchilles, A. V.; Miguel, P. J.; Vercher, E.; Martinez-Andreu, A. Isobaric Vapor-Liquid Equilibria for 1-Propanol Plus Water Plus 1-Ethyl-3-methylimidazolium Trifluoromethanesulfonate at 100 kPa. *J. Chem. Eng. Data* **2008**, *53*, 2426−2431.
(47) Garcia-Mardones, M.; Barros, A.; Bandres, I.; Artigas, H.; Lafuente, C. Thermodynamic Properties of Binary Mixtures Combining Two Pyridinium-Based Ionic Liquids and Two Alkanols. *J. Chem. Thermodyn.* **2012**, *51*, 17−24.
(48) Guo, Y. M.; Zhang, X. S.; Xu, C.; Shen, W. G. Liquid-Liquid Phase Equilibrium and Heat Capacity of Binary Solution {2-Propanol + 1-Octy1−3-methylimidazolium Hexafluorophosphate}. *J. Chem. Thermodyn.* **2017**, *105*, 434−442.
(49) Schröer, W.; Vale, V. R. Liquid-Liquid Phase Separation in Solutions of Ionic Liquids: Phase Diagrams, Corresponding State Analysis and Comparison with Simulations of the Primitive Model. *J. Phys.: Condens. Matter* **2009**, *21*, 424119.
(50) Shao, X. W.; Schröer, W.; Rathke, B. Liquid-Liquid Phase Behavior of Solutions of 1,3-Dimethylimidazolium- and 1-Methyl-3-propylimidazolium Bis((trifluoromethyl)sulphonyl)amide (C(1,3)-mimNTf(2)) in n-Alkyl Alcohols. *J. Chem. Eng. Data* **2014**, *59*, 225−233.
(51) Vale, V. R.; Will, S.; Schröer, W.; Rathke, B. The General Phase Behavior of Mixtures of 1-Alkyl-3-Methylimidazolium Bis-[(trifluoromethyl)sulfonyl]amide Ionic Liquids with n-Alkyl Alcohols. *ChemPhysChem* **2012**, *13*, 1860−1867.
(52) Vale, V. R.; Rathke, B.; Will, S.; Schröer, W. Liquid-Liquid Phase Behavior of Solutions of 1-Butyl-3-methylimidazolium Bis-((trifluoromethyl)sulfonyl)amide (C(4)mimNTf(2)) in n-Alkyl Alcohols. *J. Chem. Eng. Data* **2011**, *56*, 4829−4839.
(53) Vale, V. R.; Rathke, B.; Will, S.; Schröer, W. Liquid-Liquid Phase Behavior of Solutions of 1-Hexyl-3-methylimidazolium Bis-((trifluoromethyl)sulfonyl)amide (C(6)mimNTf(2)) in n-Alkyl Alcohols. *J. Chem. Eng. Data* **2011**, *56*, 1330−1340.
(54) Vale, V. R.; Rathke, B.; Will, S.; Schröer, W. Liquid-Liquid Phase Behavior of Solutions of 1-Dodecyl-3-methylimidazolium Bis-((trifluoromethyl)sulfonyl)amide (C(12)mimNTf(2)) in n-Alkyl Alcohols. *J. Chem. Eng. Data* **2010**, *55*, 4195−4205.
(55) Vale, V. R.; Rathke, B.; Will, S.; Schröer, W. Liquid-Liquid Phase Behavior of Solutions of 1-Octyl- and 1-Decy1−3-methylimidazolium Bis(trifluoromethylsulfonyl)imide (C(8,10)mimNTf(2)) in n-Alkyl Alcohols. *J. Chem. Eng. Data* **2010**, *55*, 2030−2038.
(56) Domanska, U.; Karpinska, M.; Wlazlo, M. Bis-(trifluoromethylsulfonyl)imide, or Dicyanamide-Based Ionic Liquids in the Liquid-Liquid Extraction of Hex-1-ene from Hexane and Cyclohexene from Cyclohexane. *J. Chem. Thermodyn.* **2017**, *105*, 375−384.
(57) Domanska, U.; Krolikowski, M. Extraction of Butan-1-ol from Water with Ionic Liquids at T = 308.15 K. *J. Chem. Thermodyn.* **2012**, *53*, 108−113.
(58) Domanska, U.; Bogel-Lukasik, E.; Bogel-Lukasik, R. 1-Octanol/Water Partition Coefficients of 1-Alkyl-3-methylimidazolium Chloride. *Chem. - Eur. J.* **2003**, *9*, 3033−3041.
(59) Rotrekl, J.; Storch, J.; Velisek, P.; Schröer, W.; Jacquemin, J.; Wagner, Z.; Husson, P.; Bendova, M. Liquid Phase Behavior in Systems of 1-Butyl-3-alkylimidazolium Bis{(trifluoromethyl)sulfonyl}imide Ionic Liquids with Water: Influence of the Structure of the C5 Alkyl Substituent. *J. Solution Chem.* **2017**, *46*, 1456−1474.
(60) Qiao, Y. X.; Ma, W. B.; Theyssen, N.; Chen, C.; Hou, Z. S. Temperature-Responsive Ionic Liquids: Fundamental Behaviors and Catalytic Applications. *Chem. Rev.* **2017**, *117*, 6881−6928.
(61) Carvalho, P. J.; Khan, I.; Morais, A.; Granjo, J. F. O.; Oliveira, N. M. C.; Santos, L. M. N. B. F.; Coutinho, J. A. P. A New Microebulliometer for the Measurement of the Vapor-Liquid Equilibrium of Ionic Liquid Systems. *Fluid Phase Equilib.* **2013**, *354*, 156−165.
(62) Andreatta, A. E.; Charnley, M. P.; Brennecke, J. F. Using Ionic Liquids to Break the Ethanol-Ethyl Acetate Azeotrope. *ACS Sustainable Chem. Eng.* **2015**, *3*, 3435−3444.
(63) Orchilles, A. V.; Miguel, P. J.; Llopis, F. J.; Vercher, E.; Martinez-Andreu, A. Influence of Some Ionic Liquids Containing the Trifluoromethanesulfonate Anion on the Vapor-Liquid Equilibria of the Acetone plus Methanol System. *J. Chem. Eng. Data* **2011**, *56*, 4430−4435.
(64) Orchilles, A. V.; Miguel, P. J.; Gonzalez-Alfaro, V.; Vercher, E.; Martinez-Andreu, A. Isobaric Vapor-Liquid Equilibria of 1-Propanol + Water plus Trifluoromethanesulfonate-Based Ionic Liquid Ternary Systems at 100 kPa. *J. Chem. Eng. Data* **2011**, *56*, 4454−4460.
(65) Orchilles, A. V.; Miguel, P. J.; Gonzalez-Alfaro, V.; Llopis, F. J.; Vercher, E.; Martinez-Andreu, A. Isobaric Vapor-Liquid Equilibria for the 1-Propanol + Water+1-Ethyl-3-methylimidazolium Dicyanamide System at 100 kPa. *J. Chem. Thermodyn.* **2017**, *113*, 116−123.
(66) Calvar, N.; Gomez, E.; Gonzalez, B.; Dominguez, A. Experimental Vapor-Liquid Equilibria for the Ternary System Ethanol + Water+1-Ethyl-3-methylpyridinium Ethylsulfate and the Corresponding Binary Systems at 101.3 kPa: Study of the Effect of the Cation. *J. Chem. Eng. Data* **2010**, *55*, 2786−2791.
(67) Li, W. X.; Sun, D. Z.; Zhang, T.; Huang, Y. H.; Zhang, L.; Zhang, Z. G. Phase Equilibrium Study of Binary and Ternary Mixtures of Ionic Liquids plus Acetone plus Methanol. *J. Chem. Eng. Data* **2014**, *59*, 3975−3981.
(68) Li, W. X.; Xu, N. N.; Xu, H. H.; Zhang, A. D.; Zhang, Z. G.; Zhang, T. Isobaric Vapor-Liquid Equilibrium for Ternary Mixtures of Acetone plus Methanol plus Ionic Liquids at 101.3 kPa. *Fluid Phase Equilib.* **2017**, *442*, 20−27.
(69) Cumplido, M. P.; Lladosa, E.; Loras, S.; Pla-Franco, J. Isobaric Vapor-Liquid Equilibria for Extractive Distillation of 1-Propanol + Water Mixture Using Thiocyanate-Based Ionic Liquids. *J. Chem. Thermodyn.* **2017**, *113*, 219−228.
(70) Safarov, J.; Kul, I.; Talibov, M.; Shahverdiyev, A.; Hassel, E. Vapor Pressures and Activity Coefficients of Methanol in Binary Mixtures with 1-Hexyl-3-methylimidazolium Bis(trifluoromethylsulfonyl)imide. *J. Chem. Eng. Data* **2015**, *60*, 1648−1663.
(71) Verevkin, S. P.; Safarov, J.; Bich, E.; Hassel, E.; Heintz, A. Thermodynamic Properties of Mixtures Containing Ionic Liquids Vapor Pressures and Activity Coefficients of n-Alcohols and Benzene in Binary Mixtures with 1-Methyl-3-butyl-imidazolium Bis-(trifluoromethyl-sulfonyl)imide. *Fluid Phase Equilib.* **2005**, *236*, 222−228.
(72) Hector, T.; Uhlig, L.; Gmehling, J. Prediction of Different Thermodynamic Properties for Systems of Alcohols and Sulfate-Based Anion Ionic Liquids Using Modified UNIFAC. *Fluid Phase Equilib.* **2013**, *338*, 135−140.
(73) Orchilles, A. V.; Miguel, P. J.; Vercher, E.; Martinez-Andreu, A. Ionic Liquids as Entrainers in Extractive Distillation: Isobaric Vapor-Liquid Equilibria for Acetone plus Methanol plus 1-Ethyl-3-methyl-imidazolium Trifluoromethanesulfonate. *J. Chem. Eng. Data* **2007**, *52*, 141−147.
(74) Han, J. L.; Lei, Z. G.; Dai, C. N.; Li, J. S. Vapor Pressure Measurements for Binary Mixtures Containing Ionic Liquid and Predictions by the Conductor-Like Screening Model for Real Solvents. *J. Chem. Eng. Data* **2016**, *61*, 1117−1124.

DOI: 10.1021/acs.jpcb.8b03278
J. Phys. Chem. B 2018, 122, 6017−6032

(75) Calvar, N.; Gonzalez, B.; Gomez, E.; Dominguez, A. Vapor-Liquid Equilibria for the Ternary System Ethanol + Water+1-Ethyl-3-methylimidazolium Ethylsulfate and the Corresponding Binary Systems Containing the Ionic Liquid at 101.3 kPa. *J. Chem. Eng. Data* **2008**, *53*, 820−825.
(76) Zhu, J. J.; Li, Q. S.; Li, M. T.; Song, X. L.; Tang, H. J.; Liu, Y. D. The Isobaric Vapor Liquid Equilibria of Ethyl Acetate plus Acetonitrile plus Bis(trifluoromethylsulfonyl)imide-Based Ionic Liquids at 101.3 kPa. *Fluid Phase Equilib.* **2016**, *425*, 289−296.
(77) Rarey, J.; Gmehling, J. Computer-Controlled Static Ebulliometer for Determination of Reliable Vapor-Liquid Equilibrium Data. *Chem. Ing. Tech.* **1993**, *65*, 308−310.
(78) Ambrose, D.; Townsend, R. 681. Thermodynamic Properties of Organic Oxygen Compounds. Part IX. The Critical Properties and Vapour Pressures, Above Five Atmospheres, of Six Aliphatic Alcohols. *J. Chem. Soc.* **1963**, *0*, 3614−3625.
(79) Cottrell, F. G. On The Determination of Boiling Points of Solutions. *J. Am. Chem. Soc.* **1919**, *41*, 721−729.
(80) Gillespie, D. T. C. Vapor-Liquid Equilibrium Still from Miscible Liquids. *Ind. Eng. Chem., Anal. Ed.* **1946**, *18*, 575−577.
(81) Hala, E.; Wichterle, I.; Polák, J.; Boublik, T. *Vapour-Liquid Equilibrium Data at Normal Pressures*; Pergamon Press: Oxford, London, Edinburgh, 1968.
(82) Wichterle, I.; Hala, E. Semimicrodetermination of Vapor-Liquid Equilibrium. *Ind. Eng. Chem. Fundam.* **1963**, *2*, 155−157.
(83) Stage, H.; Müller, E.; Gemmeker, L. Neue Umlaufapparatur zur Vermessung von Dampf-Flüssigkeits-Phasengleichgewichten. *Chemiker-Ztg. - Chemische Apparatur* **1961**, *85*, 387−395.
(84) Röck, H. *Destillation im Laboratorium - Extraktive und Azeotrope Destillation*. Dr. Dietrich Steinkopff Verlag: Darmstadt, 1960; Vol. *5*.
(85) Stage, H.; Fischer, W. G. Verbesserte Labodest - Umlaufapparaturen zur Vermessung von Dampf-Flüssigkeits-Phasengleichgewichten. *G.I.T. Fachzeitschrift für das Laboratorium* **1968**, *12*, 1167−1173.
(86) Blas, F. J.; Vega, L. F. Thermodynamic Behaviour of Homonuclear and Heteronuclear Lennard-Jones Chains with Association Sites from Simulation and Theory. *Mol. Phys.* **1997**, *92*, 135−150.
(87) Blas, F. J.; Vega, L. F. Prediction of Binary and Ternary Diagrams Using the Statistical Associating Fluid Theory (SAFT) Equation of State. *Ind. Eng. Chem. Res.* **1998**, *37*, 660−674.
(88) Mac Dowell, N.; Llovell, F.; Sun, N.; Hallett, J. P.; George, A.; Hunt, P. A.; Welton, T.; Simmons, B. A.; Vega, L. F. New Experimental Density Data and Soft-SAFT Models of Alkylimidazolium (C(n)C(1)-im (+)) Chloride (Cl-), Methylsulfate (MeSO4 (−)), and Dimethylphosphate (Me2PO4 (−)) Based Ionic Liquids. *J. Phys. Chem. B* **2014**, *118*, 6206−6221.
(89) Oliveira, M. B.; Crespo, E. A.; Llovell, F.; Vega, L. F.; Coutinho, J. A. P. Modeling the Vapor-Liquid Equilibria and Water Activity Coefficients of Alternative Refrigerant-Absorbent Ionic-Liquid Water Pairs for Absorption Systems. *Fluid Phase Equilib.* **2016**, *426*, 100−109.
(90) Oliveira, M. B.; Llovell, F.; Coutinho, J. A. P.; Vega, L. F. Modeling the NTf2 Pyridinium Ionic Liquids Family and Their Mixtures with the Soft Statistical Associating Fluid Theory Equation of State. *J. Phys. Chem. B* **2012**, *116*, 9089−9100.
(91) Vega, L. F.; Vilaseca, O.; Llovell, F.; Andreu, J. S. Modeling Ionic Liquids and the Solubility of Gases in Them: Recent Advances and Perspectives. *Fluid Phase Equilib.* **2010**, *294*, 15−30.
(92) Hendriks, E. M. Applied Thermodynamics in Industry, a Pragmatic Approach. *Fluid Phase Equilib.* **2011**, *311*, 83−92.
(93) Chapman, W. G.; Gubbins, K. E.; Jackson, G.; Radosz, M. SAFT - Equation-of-State Solution Model for Associating Fluids. *Fluid Phase Equilib.* **1989**, *52*, 31−38.
(94) Chapman, W. G.; Gubbins, K. E.; Jackson, G.; Radosz, M. New Reference Equation of State for Associating Liquids. *Ind. Eng. Chem. Res.* **1990**, *29*, 1709−1721.
(95) Wertheim, M. S. Fluids with Highly Directional Attractive Forces 0.1. Statistical Thermodynamics. *J. Stat. Phys.* **1984**, *35*, 19−34.
(96) Wertheim, M. S. Fluids with Highly Directional Attractive Forces 0.2. Thermodynamic Perturbation-Theory and Integral-Equations. *J. Stat. Phys.* **1984**, *35*, 35−47.
(97) Wertheim, M. S. Fluids with Highly Directional Attractive Forces 0.3. Multiple Attraction Sites. *J. Stat. Phys.* **1986**, *42*, 459−476.
(98) Wertheim, M. S. Fluids with Highly Directional Attractive Forces 0.4. Equilibrium Polymerization. *J. Stat. Phys.* **1986**, *42*, 477−492.
(99) Vega, L. F.; Llovell, F. Review and New Insights into the Application of Molecular-Based Equations of State to Water and Aqueous Solutions. *Fluid Phase Equilib.* **2016**, *416*, 150−173.
(100) Pereira, L. M. C.; Martins, V.; Kurnia, K. A.; Oliveira, M. B.; Dias, A. M. A.; Llovell, F.; Vega, L. F.; Carvalho, P. J.; Coutinho, J. A. P. High Pressure Solubility of CH4, N2O and N-2 in 1-Butyl-3-methylimidazolium Dicyanamide: Solubilities, Selectivities and Soft-SAFT Modeling. *J. Supercrit. Fluids* **2016**, *110*, 56−64.
(101) Pereira, L. M. C.; Oliveira, M. B.; Dias, A. M. A.; Llovell, F.; Vega, L. F.; Carvalho, P. J.; Coutinho, J. A. P. High Pressure Separation of Greenhouse Gases from Air with 1-Ethyl-3-methylimidazolium Methylphosphonate. *Int. J. Greenhouse Gas Control* **2013**, *19*, 299−309.
(102) Pereira, L. M. C.; Oliveira, M. B.; Llovell, F.; Vega, L. F.; Coutinho, J. A. P. Assessing the N2O/CO2 High Pressure Separation Using Ionic Liquids with the Soft-SAFT EoS. *J. Supercrit. Fluids* **2014**, *92*, 231−241.
(103) Oliveira, M. B.; Dominguez-Perez, M.; Freire, M. G.; Llovell, F.; Cabeza, O.; Lopes-da-Silva, J. A.; Vega, L. F.; Coutinho, J. A. P. Surface Tension of Binary Mixtures of 1-Alkyl-3-methylimidazolium Bis-(trifluoromethylsulfonyl)imide Ionic Liquids: Experimental Measurements and Soft-SAFT Modeling. *J. Phys. Chem. B* **2012**, *116*, 12133−12141.
(104) Llovell, F.; Vega, L. F. Global Fluid Phase Equilibria and Critical Phenomena of Selected Mixtures Using the Crossover Soft-SAFT Equation. *J. Phys. Chem. B* **2006**, *110*, 1350−1362.
(105) Jiang, Y. P.; Nadolny, H.; Kashammer, S.; Weibels, S.; Schröer, W.; Weingärtner, H. The Ion Speciation of Ionic Liquids in Molecular Solvents of Low and Medium Polarity. *Faraday Discuss.* **2012**, *154*, 391−407.
(106) Schröer, W. A Short History of Phase Transitions in Ionic Fluids. *Contrib. Plasma Phys.* **2012**, *52*, 78−88.
(107) Weingärtner, H.; Kleemeier, M.; Wiegand, S.; Schröer, W. Coulombic and Non-Coulombic Contributions to the Criticality of Ionic Fluids - An Experimental Approach. *J. Stat. Phys.* **1995**, *78*, 169−196.
(108) Weingärtner, H.; Schröer, W. Criticality of Ionic Fluids. *Adv. Chem. Phys.* **2007**, *116*, 1−66.
(109) Weingärtner, H.; Weiss, V. C.; Schröer, W. Ion Association and Electrical Conductance Minimum in Debye-Huckel-Based Theories of the Hard Sphere Ionic Fluid. *J. Chem. Phys.* **2000**, *113*, 762−770.
(110) Johnson, J. K.; Zollweg, J. A.; Gubbins, K. E. The Lennard-Jones Equation of State Revisited. *Mol. Phys.* **1993**, *78*, 591−618.
(111) Pamies, J. C.; Vega, L. F. Vapor-Liquid Equilibria and Critical Behavior of Heavy n-Alkanes Using Transferable Parameters from the Soft-SAFT Equation of State. *Ind. Eng. Chem. Res.* **2001**, *40*, 2532−2543.
(112) Oliveira, M. B.; Llovell, F.; Coutinho, J. A. P.; Vega, L. F. New Procedure for Enhancing the Transferability of Statistical Associating Fluid Theory (SAFT) Molecular Parameters: The Role of Derivative Properties. *Ind. Eng. Chem. Res.* **2016**, *55*, 10011−10024.
(113) Llovell, F.; Vilaseca, O.; Jung, N.; Vega, L. F. Water+1-Alkanol Systems: Modeling the Phase, Interface and Viscosity Properties. *Fluid Phase Equilib.* **2013**, *360*, 367−378.
(114) Pàmies, J. C. *Bulk and Interfacial Properties of Chain Fluids: A Molecular Modelling Approach*; Universitat Rovira i Virgili, Tarragona, 2003.
(115) Vega, L. F.; Llovell, F.; Blas, F. J. Capturing the Solubility Minima of n-Alkanes in Water by Soft-SAFT. *J. Phys. Chem. B* **2009**, *113*, 7621−7630.
(116) Huang, S. H.; Radosz, M. Equation of State for Small, Large, Polydisperse, and Associating Molecules. *Ind. Eng. Chem. Res.* **1990**, *29*, 2284−2294.
(117) Poling, B. E.; Prausnitz, J. M.; O'Connell, J. P. *The Properties of Gases and Liquids*, 5th ed.; The McGraw-Hill Companies, Inc.: Bangkok, Bogota, Caracas, 2001.

DOI: 10.1021/acs.jpcb.8b03278
J. Phys. Chem. B 2018, 122, 6017−6032

(118) Rowley, R. L.; Wilding, W. V.; Oscarson, J. L.; Yang, Y.; Zundel, N. A.; Daubert, T. E.; Danner, R. P. *DIPPR Data Compilation of Pure Chemical Properties*. In Properties, D. I. f. P., Ed. AIChE: New York, 2007.
(119) *Evaluation of measurement data - Guide to the expression of uncertainty in measurement JCGM 100:2008*. Bureau International des Poids et Mesures (BIPM): 2008.
(120) Stull, D. R. Vapor Pressure of Pure Substances - Inorganic Compounds. *Ind. Eng. Chem.* **1947**, *39*, 540−550.
(121) Liu, C.-T.; Lindsay, W. T. Vapor Pressure of Deuterated Water from 106 to 300.Deg. *J. Chem. Eng. Data* **1970**, *15*, 510−513.
(122) Ambrose, D.; Sprake, C. H. S. Thermodynamic Properties of Organic Oxygen Compounds XXV. Vapour Pressures and Normal Boiling Temperatures of Aliphatic Alcohols. *J. Chem. Thermodyn.* **1970**, *2*, 631−645.
(123) Ambrose, D.; Sprake, C. H. S.; Townsend, R. Thermodynamic Properties of Organic Oxygen Compounds XXXVII. Vapour Pressures of Methanol, Ethanol, Pentan-1-ol, and Octan-1-ol from the Normal Boiling Temperature to the Critical Temperature. *J. Chem. Thermodyn.* **1975**, *7*, 185−190.
(124) Kemme, H. R.; Kreps, S. I. Vapor Pressure of Primary n-Alkyl Chlorides and Alcohols. *J. Chem. Eng. Data* **1969**, *14*, 98−102.
(125) Hessel, D.; Geiseler, G. Über die Druckabhängigkeit des Heteroazeotropen Systems n-Butanol/Wasser. *Z. Phys. Chem.* **1965**, *229*, 199−209.
(126) Elshwishin, A. O. O. Untersuchung des Flüssig-Flüssig Phasenübergangs von Lösungen Ionischer Flüssigkeiten mit dem Trifluormethylsulfonat Anion. Inaugural Dissertation, Universität Bremen, Bremen, 2011.

DOI: 10.1021/acs.jpcb.8b03278
J. Phys. Chem. B 2018, 122, 6017−6032